WILEY

Parameterizing robust manipulator controllers under approximate inverse dynamics: A double-Youla approach

Stefan R. Friedrich[1,2] | **Martin Buss**[1,2]

[1]Department of Electrical and Computer Engineering, Chair of Automatic Control Engineering, Technical University of Munich, Munich, Germany

[2]Institute for Advanced Study, Technical University of Munich, Garching, Germany

Correspondence
Stefan R. Friedrich, Department of Electrical and Computer Engineering, Chair of Automatic Control Engineering, Technical University of Munich, Theresienstr. 90, 80333 Munich, Germany.
Email: s.friedrich@tum.de

Funding information
ERC Advanced, Grant/Award Number: 267877; Technische Universität München, Institute for Advanced Study

Summary

We consider the goal of ensuring robust stability when a given manipulator feedback control law is modified online, for example, to safely improve the performance by a learning module. To this end, the factorization approach is applied to both the plant and controller models to characterize robustly stabilizing controllers for rigid-body manipulators under approximate inverse dynamics control. Outer-loop controllers to stabilize the nonlinear uncertain loop that results from approximate inverse dynamics are often derived by lumping uncertainty in a single term and subsequent analysis of the error system. Here, by contrast, the well-known norm bounds of these uncertain dynamics are first recast into a generalized plant configuration that preserves the characteristic uncertainty structure. Then, the overall loop uncertainty is expressed with respect to the nominal outer-loop feedback controller by means of an uncertain dual-Youla operator. Therefore, using the dual-Youla parameterization, we provide a novel way to rigorously quantify permissible perturbations of robot manipulator feedforward/feedback controllers. The method proposed in this paper does not constitute another robust control law for rigid-body manipulators, but rather a characterization of a set of robustly stabilizing controllers. The resulting double-Youla parameterization for the control of robot manipulators is amenable to numerous advanced design methods. The result is thoroughly discussed by a planar elbow manipulator and exemplified with a six-degree-of-freedom robot scenario with varying payload.

KEYWORDS

approximate inverse dynamics, dual-Youla parameterization, robust robot manipulator control, robust/adaptive control, uncertainty quantification

1 | INTRODUCTION

Operating conditions of robot manipulators change over time, impairing the control performance, for example, by wear, varying load, etc. To adapt the controller to such situations, a variety of data-driven methods have been proposed in the literature, including adaptive and learning control.[1-4] In practice, however, very simple feedback controllers and model-based architectures are prevalent.
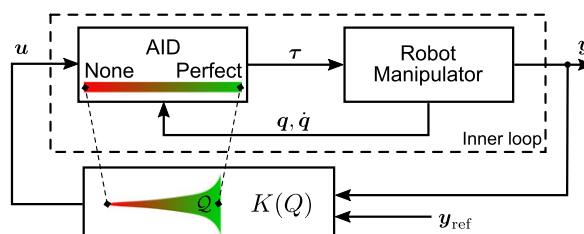
On the one hand, if the complete dynamic model is available, feedback linearization can be applied. On the other hand, simple, completely model free controllers are ubiquitous, most prominently, the popular proportional-derivative (PD) controller. Both may be interpreted as two extremes on the spectrum of approximate inverse dynamics (AID) controllers: ideal linearization is theoretically achieved if the model is perfect; if, on the contrary, there simply is no dynamical model in the controller, only the PD action of the outer loop remains. In this article, we consider the following question. Given a robot manipulator under AID control, *how* and *how much* can the outer-loop controller be modified during operation without compromising stability? Answering this question ultimately allows to use for online control performance enhancement methods that are otherwise hard to employ in a strict robust stability framework, eg, black-box optimization or reinforcement learning.

It is intuitively clear that the worse the controller is informed about the dynamic characteristics of the controlled robot, the harder it will be to provide stability guarantees when the controller is modified during operation. This situation is depicted in Figure 1 and motivates this article: We provide a method to *quantify* this trade-off. We then characterize a *set* of robustly stabilizing controllers $\mathcal{K}_R$, ie, all controllers contained in $\mathcal{K}_R$ stabilize the uncertain nonlinear inner loop resulting from a particular AID situation. Interestingly, not only the model accuracy but also the nominal outer-loop controller K influence the amount of apparent uncertainty in the loop. Only comparatively recently, Bascetta and Rocco[5] have reformulated the robust control of rigid manipulators to account for this issue, after it had not been considered by the most common robust robot control methods.[1-4] The new framework proposed in this article provides a unified perspective and constitutes a tool to explore freedom in controller (re)tuning, given a simplified model of the robot manipulator and a nominal outer-loop controller K.

Central to our method is a Q-parameterization (viz, Youla-Kučera parameterization due to the original developments in the works of Youla et al[6] and Kučera[7]) of stabilizing controllers and the dual S-parameterization of plants stabilized by a controller.[8] The primary parameterization was already applied to the robust linear design of robot controllers around 30 years ago,[9] known in robotics as the stable factorization approach.[9,10] Our interest in extending this approach is due to the beneficial stability and robustness properties obtained by a Q-parameterization: Our recent work[11] suggests that such a parameterization is very helpful to leverage machine learning also in a feedback configuration, that is, in closed loop and on hardware. Inherently, the question is raised of how much feedback controller modification is admissible, given the effect of neglected uncertainties in the closed-loop system. The dual-Youla parameter S is needed to answer this question and there appears to be a gap in the literature of how to utilize the dual parameterization[12] for the control of robot manipulators. The following novel methodological contributions are given.

(i) A generalized plant description of the rigid-body robot manipulator under AID control is formulated, such that the sources of uncertainty remain separated and the outer-loop controller K is left undetermined.

(ii) Next, a dual-Youla parameterization is derived to quantify the uncertainty occurring by the interplay of neglected manipulator dynamics in the inner loop and the outer-loop controller K. Opposed to the works of Bascetta and Rocco[5] and Spong and Vidyasagar,[9] our approach allows for a general control configuration and the sources of uncertainty are kept separated throughout. Hence, we propose a unified framework to rigorously assess the uncertainty arising in the closed-loop system.

(iii) Our main result is a general parameterization of robustly stabilizing two-degree-of-freedom (DoF) (feedforward/feedback) controllers for rigid-body manipulators under AID control that is amenable to a variety of control design

FIGURE 1 The goal of this article is to parameterize a set of robustly stabilizing feedback controllers for rigid-body robot manipulators. To this end, a general approximate inverse dynamics (AID) controller is considered in the inner loop that may range from a perfect inverse dynamics model to none at all. An outer-loop feedback controller K be given that stabilizes the loop but may not yet yield satisfactory performance. Therefore, in general, one can augment K by some stable parameter $Q \in \mathcal{Q} \subseteq \mathcal{RH}_\infty$. However, if the dynamic model of in the inner AID loop is imperfect, only a subset $\mathcal{Q} \subset \mathcal{RH}_\infty$ is admissible to preserve the stability of the overall loop. In this article, the set $\mathcal{Q}$ and the controller parameterization $K(Q)$ are characterized such that various advanced design methods can be used for robust controller performance enhancement [Colour figure can be viewed at wileyonlinelibrary.com]

methods (learning, gain scheduling, etc). To this end, the worst-case uncertainty measure from (ii) is employed in a *double-Youla* parameterization, effectively tightening the set of nominally stabilizing controllers for the ideal double integrator system to the corresponding subset of robustly stabilizing controllers.

(iv) The derivation offers several new developments of relevance to the broader control community beyond the scope of robotics. In particular:

(a) A state-space realization for the dual-Youla parameter is derived for nondynamic metric-bounded uncertainty, given an arbitrary linear controller and a strictly proper plant.

(b) We specialize the result to a double-Youla parameterization based on a static central controller and discuss a choice of the gain design parameter such that the results are further simplified.

The remainder of this article is structured as follows. We first introduce the methods underlying our work in Section 2. The main result is given in Section 3, a general double-Youla parameterization for robot manipulators under AID control; the specialization using a static nominal controller is then reported in Section 4. In Section 5, the results are exemplified and thoroughly discussed by means of a planar elbow manipulator and a PUMA P560 robot model with six DoFs. The proofs and some technical details are provided in the Appendix.

Notation. Lowercase boldface letters are for vectors ($\boldsymbol{x}$), matrices ($\boldsymbol{M}$) are written in capital bold letters, sets ($\mathcal{S}$) are calligraphic, transfer operators (G) that define input/output relations are in standard capital letters, and $\left[\begin{array}{c|c} A & B \\ \hline C & D \end{array}\right]$ stands for a state-space realization. The symbol $\triangleq$ means equality by definition. The set of nonnegative real numbers is $\mathbb{R}_0^+$ and the Euclidean space of vectors of dimension n is denoted $\mathbb{R}^n$, with the 2-norm $\|\boldsymbol{x}\| = \sqrt{\sum_{i=1}^n |x_i|^2}$. The corresponding induced matrix norm of an $n \times n$ matrix $\boldsymbol{M}$ is written $\|\boldsymbol{M}\|$. The vertical concatenation of two column vectors $\boldsymbol{x}_1, \boldsymbol{x}_2$ is denoted $\text{col}(\boldsymbol{x}_1 \boldsymbol{x}_2) \triangleq [\boldsymbol{x}_1^\top, \boldsymbol{x}_2^\top]^\top$. A symmetric positive definite matrix $\boldsymbol{M} = \boldsymbol{M}^\top$ is written $\boldsymbol{M} \succ 0$. The set of γ-bounded $n \times m$ real matrices w.r.t. the induced p-norm is $\mathcal{B}_p^{n \times m}(\gamma) \triangleq \{\boldsymbol{M} : \boldsymbol{M} \in \mathbb{R}^{n \times m}, \|\boldsymbol{M}\|_p \leq \gamma\}$. The set $\mathcal{C}^2$ consists of twice continuously differentiable functions on $\mathbb{R}$. The set of all piecewise continuous integrable functions $\boldsymbol{x} : \mathbb{R}_0^+ \mapsto \mathbb{R}^n$ is the Lebesgue space $\mathcal{L}_p$ for $1 \leq p < \infty$ with norm $\|\boldsymbol{x}\|_{\mathcal{L}_p} = (\int_0^\infty \|\boldsymbol{x}(t)\|^p dt)^{1/p} < \infty$, and ℓ_p denotes the analogous discrete-time norms. Furthermore, $\boldsymbol{x}(t) \in \mathcal{L}_\infty(\mathbb{R}_0^+, \mathbb{R}^n)$ is the space of uniformly bounded functions with $\|\boldsymbol{x}(t)\|_{\mathcal{L}_\infty} < \infty$. We use the convention that if $G(s)$ is a transfer matrix and $\boldsymbol{u} = \boldsymbol{u}(t)$ is a Laplace transformable signal, then by $G\boldsymbol{u}$ the signal $(\boldsymbol{g} * \boldsymbol{u})(t)$ is meant, where $\boldsymbol{g}(t)$ is the impulse response of $G(s)$ and $*$ denotes the convolution operator, with the technical distinction being given from the context. The space $\mathcal{RH}_\infty$ denotes the set of all proper and real $n \times m$ rational stable transfer matrices $G(s)$ and the associated $\mathcal{H}_\infty$ norm is $\|G(s)\|_\infty \triangleq \sup_{\omega \in \mathbb{R}} \bar{\sigma}(G(j\omega))$, where $\bar{\sigma}$ denotes the largest singular value. If G is a nonlinear mapping, by $\|G\|_\infty$ the induced $\mathcal{L}_2$ gain of G is meant. The feedback interconnection of two systems G_1 and G_2 through common input/output variables is written (G_1, G_2). A lower linear fractional transformation of a partitioned operator $G = \begin{bmatrix} G_{11} & G_{12} \\ G_{21} & G_{22} \end{bmatrix} \in \mathcal{RH}_\infty$ with another mapping K is written $\mathcal{F}_\ell(G, K) \triangleq G_{11} + G_{12}K(I - G_{22}K)^{-1}G_{21}$, whereas the upper fractional transformation is $\mathcal{F}_u(G, \Delta) \triangleq G_{22} + G_{21}\Delta(I - G_{11}\Delta)^{-1}G_{12}$. The transformations are well defined if and only if the well-posedness condition is satisfied.

2 | REVIEW OF UNDERLYING CONCEPTS

2.1 | Rigid-body manipulator dynamics and tracking control

We consider a rigid-body robot manipulator with n links, described by the standard Euler-Lagrange model[1-3]

$$\boldsymbol{M}(\boldsymbol{q}(t))\ddot{\mathbf{q}}(t) + \boldsymbol{n}(\boldsymbol{q}(t), \dot{\boldsymbol{q}}(t)) = \tau(t) + \tau_{\text{dist}}(t), \tag{1}$$

$$\boldsymbol{n}(\boldsymbol{q}(t), \dot{\boldsymbol{q}}(t)) = \boldsymbol{C}(\boldsymbol{q}(t), \dot{\boldsymbol{q}}(t))\dot{\boldsymbol{q}}(t) + \boldsymbol{f}(\dot{\boldsymbol{q}}(t)) + \boldsymbol{g}(\boldsymbol{q}(t)), \tag{2}$$

where $\boldsymbol{q}(t) \in \mathbb{R}^n$ is the vector of generalized coordinates (representing joint positions), $\tau \in \mathbb{R}^n$ is the input vector of generalized force (torque), $\boldsymbol{M}(\boldsymbol{q}) \in \mathbb{R}^{n \times n}, \boldsymbol{M}(\boldsymbol{q}) \succ 0$ is the inertia matrix, and $\boldsymbol{n} \in \mathbb{R}^n$ is a vector that summarizes the vector of Coriolis and centrifugal terms $\boldsymbol{C}(\boldsymbol{q}(t), \dot{\boldsymbol{q}}(t))\dot{\boldsymbol{q}}(t) \in \mathbb{R}^n$, the friction terms $\boldsymbol{f}(\dot{\boldsymbol{q}}(t)) \in \mathbb{R}^n$, and the gravitational terms $\boldsymbol{g}(\boldsymbol{q}(t)) \in \mathbb{R}^n$. It is assumed that the input disturbance $\tau_{\text{dist}}(t)$ is a Lebesgue measurable function. The state of the system

is denoted $x(t) = \text{col}(q(t), \dot{q}(t))$. Given a desired path in joint space $q_{\text{d}}(t) \in C^2$, $q_{\text{d}}, \dot{q}_{\text{d}}, \ddot{q}_{\text{d}} \in \mathcal{L}_\infty(\mathbb{R}_+, \mathbb{R}^n)$, the tracking error is formed as $e(t) = \text{col}(e_1(t), e_2(t)) = \text{col}(q_{\text{d}}(t) - q(t), \dot{q}_{\text{d}}(t) - \dot{q}(t))$. The measurement available for feedback is assumed as $\hat{q}(t) = q + w_1(t)$, $\dot{\hat{q}}(t) = \dot{q}(t) + w_2(t)$, where $w(t)$ represents measurement uncertainty. The goal of tracking control is to find a controller generating $\tau(t)$ such that $e(t)$ vanishes. For the sake of readability, we henceforth drop the dependency on time t where it is unambiguously clear from the context.

2.2 | Control of rigid manipulators using AID

The parameters of (1) are in pratice not known exactly. The *approximate* or *realistic* inverse dynamics control[2,3] therefore attempts to cancel the nonlinearities of (1) by feedback linearization based on the measured quantities and an available model of the dynamic parameters, denoted by $(\hat{\cdot})$:

$$\tau = \hat{M}(\hat{q})u + \hat{n}(\hat{q}), \qquad \text{where} \quad \hat{n}(\hat{q}, \dot{\hat{q}}) = \hat{C}(\hat{q}, \dot{\hat{q}})\dot{\hat{q}} + \hat{f}(\dot{\hat{q}}) + \hat{g}(\hat{q}). \tag{3}$$

The available model parameters may have been obtained by estimations (eg, due to unknown load) or approximations (unknown dynamic model, simplified models, etc). The error quantities are denoted using $\widetilde{(\cdot)}$ as

$$\widetilde{M}(q, \hat{q}) = \hat{M}(\hat{q}) - M(q), \qquad \widetilde{n}(\hat{q}, \dot{\hat{q}}, q, \dot{q}) = \hat{n}(\hat{q}, \dot{\hat{q}}) - n(q, \dot{q}). \tag{4}$$

The dynamics given by application of the control law (3) to the system (1) is referred to as *inner loop*, and the vector $u \in \mathbb{R}^n$ is the new control input that is to be determined by an outer loop. Clearly, if $\widetilde{M} \equiv 0$, $\widetilde{n} \equiv 0$, (3) achieves a perfect feedback linearization and the minimum-phase nonlinear robot equations (1) are turned into a set of double integrators. Thus, a common choice to stabilize the resulting system is a linear state feedback with positive definite gain matrices $K_{\text{P}}, K_{\text{D}} \in \mathbb{R}^{n \times n}, K_{\text{P}}, K_{\text{D}} \succ 0$ in the outer loop. The control law

$$u = [K_{\text{P}} \; K_{\text{D}}]e \tag{5}$$

then effectively acts as a PD controller.

In the realistic situation, however, the control law (3) inserted into (1) yields the following *perturbed double integrator*:

$$\ddot{q} = (I + \Delta_{\text{M}})u + \psi, \quad \text{where} \tag{6}$$

$$\Delta_{\text{M}} = M(q)^{-1}\widetilde{M}(q, \hat{q}) = M(q)^{-1}\hat{M}(\hat{q}) - I, \tag{7}$$

$$\psi = M(q)^{-1}\widetilde{n}(\hat{q}, \dot{\hat{q}}, q, \dot{q}) + M(q)^{-1}\tau_{\text{dist}}(t). \tag{8}$$

Robust AID controller design thus amounts to selecting u in the outer loop that rejects the inverse additive disturbance ψ, subject to being robust w.r.t. the multiplicative input uncertainty Δ_{M} caused by an inaccurate inertia matrix estimate $\hat{M}$. Hence, *controller design* in the following refers to the *outer-loop* controller generating u.

2.3 | Manipulator norm bounds

A number of norm bounds are routinely assumed for the system (1)-(2) as summarized in Appendix A. Moreover, the accuracy of the dynamical model is assumed to fulfill the following properties.

Assumption 1 (Model approximation).

1. There exists a constant $\alpha > 0$ such that, for all $q \in \mathbb{R}^n$,

$$\|\Delta_{\text{M}}\| = \|M(q)^{-1}\hat{M}(\hat{q}) - I\| \le \alpha. \tag{9}$$

For the analysis in this paper, it is not necessarily required that $\alpha < 1$ as in the works of Bascetta and Rocco[5] and Spong and Vidyasagar.[9] It will be shown, however, that robust performance enhancement is feasible only if $\alpha < 1$.

2. There exists a function $\Phi : \mathbb{R} \mapsto \mathbb{R}$ such that, $\forall \boldsymbol{x}, \hat{\boldsymbol{x}} \in \mathbb{R}^{2n} : \|\widetilde{\boldsymbol{n}}(\hat{\boldsymbol{q}}, \dot{\hat{\boldsymbol{q}}}, \boldsymbol{q}, \dot{\boldsymbol{q}})\| \leq \Phi(\|\boldsymbol{x}\|)$. The reader is referred to the work of Rocco[13] for details and to the work of Grimm[14] for computational procedures to obtain numeric values. In this article, the bound is taken as

$$\Phi(\|\boldsymbol{x}\|) = \alpha_0 + \alpha_1 \|\boldsymbol{x}\|. \tag{10}$$

2.4 | Controller parameterization by factorization

In this section, we provide a concise summary of the plant/controller factorization[10] approach central to this article. The resulting Q-parameterization is ubiquitously used in control theory, eg, in robust control,[15,16] computer-aided design,[17] gain scheduling,[18,19] model predictive,[20] hybrid,[21] and adaptive[22-24] control. For a general introductory exposition, the reader is referred to the work of Anderson.[8] The factorization approach has been introduced to the robust control of robots in the work of Spong and Vidyasagar[9] in a one-DoF controller design and in the work of Sugie et al[25] for a two-DoF controller design, and is nowadays covered in textbooks[4,26] as well. Proceeding in state space, our notation is along the lines of the work of Tay et al.[22]

Consider the system G with state $\boldsymbol{x}_G \in \mathbb{R}^{n_x}$,

$$G : \left[\begin{array}{c|cc} \boldsymbol{A} & \boldsymbol{B}_w & \boldsymbol{B}_u \\ \hline \boldsymbol{C}_z & \boldsymbol{D}_{zw} & \boldsymbol{D}_{zu} \\ \boldsymbol{C}_y & \boldsymbol{D}_{yw} & \boldsymbol{D}_{yu} \end{array} \right], \quad \boldsymbol{x}_G(0) = \boldsymbol{x}_{G,0}, \tag{11}$$

such that exogenous signals $\boldsymbol{w} \in \mathbb{R}^{n_w}$ (reference signals, disturbances, noise) and control inputs $\boldsymbol{u} \in \mathbb{R}^{n_u}$ are mapped to the outputs $\boldsymbol{y} \in \mathbb{R}^{n_y}$ (measurements available for control) and the performance signals $\boldsymbol{z} \in \mathbb{R}^{n_z}$ (signals to be controlled):

$$\begin{bmatrix} \boldsymbol{z} \\ \boldsymbol{y} \end{bmatrix} = \begin{bmatrix} G_{11} & G_{12} \\ G_{21} & G_{22} \end{bmatrix} \begin{bmatrix} \boldsymbol{w} \\ \boldsymbol{u} \end{bmatrix}.$$

Let $G_{11}, G_{12}, G_{21} \in \mathcal{RH}_\infty$, ie, be rational proper asymptotically stable transfer function matrices. Then, internal stability of the system is given if and only if the feedback loop that is formed by $G_0 = G_{22}(s) = \boldsymbol{C}_y(s\boldsymbol{I} - \boldsymbol{A})^{-1}\boldsymbol{B}_u + \boldsymbol{D}_{yu}$ and a controller K_0 is well-posed and internally stable (Figure 2A).

2.4.1 | Youla parameterization

To parameterize all stabilizing controllers, G_0 and K_0 are written in terms of double coprime factorizations

$$G_0 = \tilde{M}_0^{-1}\tilde{N}_0 = N_0 M_0^{-1} \text{ and } K_0 = \tilde{V}_0^{-1}\tilde{U}_0 = U_0 V_0^{-1}, \text{ where } N_0, M_0, \tilde{N}_0, \tilde{M}_0, V_0, U_0, \tilde{V}_0, \tilde{U}_0 \in \mathcal{RH}_\infty, \tag{12}$$

such that the left $(\tilde{\cdot})$ and right $(\cdot)$ factors have no unstable pole-zero cancellations, ie, chosen to satisfy the double Bezout identity

$$\begin{bmatrix} \tilde{V}_0 & -\tilde{U}_0 \\ -\tilde{N}_0 & \tilde{M}_0 \end{bmatrix} \begin{bmatrix} M_0 & U_0 \\ N_0 & V_0 \end{bmatrix} = \begin{bmatrix} M_0 & U_0 \\ N_0 & V_0 \end{bmatrix} \begin{bmatrix} \tilde{V}_0 & -\tilde{U}_0 \\ -\tilde{N}_0 & \tilde{M}_0 \end{bmatrix} = \begin{bmatrix} I & 0 \\ 0 & I \end{bmatrix}. \tag{13}$$

The following result is summarized, eg, from Th. 12.17 in the work of Zhou et al.[15]

Proposition 1 (Q-parameterization). *Given coprime factorizations (12) of the plant and the controller that fulfill (13), the set $\mathcal{K}$ of stabilizing controllers for G_0 can be characterized in terms of arbitrary stable Q as $\mathcal{K} = \{K(Q) \mid Q \in \mathcal{Q} \subseteq \mathcal{RH}_\infty\}$,*

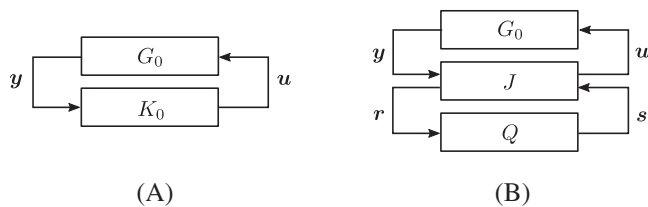$$K(Q) = U(Q)V(Q)^{-1}, \text{ where } U(Q) = U_0 + M_0 Q, \quad V(Q) = V_0 + N_0 Q \tag{14}$$

(A)

(B)

FIGURE 2 Reformulation of a feedback loop in terms of a lower fractional transformation of a stabilizing controller and a stable parameter system Q. A, Nominal controller; B, Q-parameterization

to obtain a right-factored form, or

$$K(Q) = \tilde{V}^{-1}(Q)\tilde{U}(Q), \text{ where } \tilde{V}(Q) = \tilde{V}_0 + Q\tilde{N}_0, \quad \tilde{U}(Q) = \tilde{U}_0 + Q\tilde{M}_0 \tag{15}$$

for a left stable linear fractional form. Reformulating from the definition, by the Bezout identity, we also have

$$K(Q) = \tilde{V}_0^{-1}\tilde{U}_0 + \tilde{V}_0^{-1}Q\left(I + V_0^{-1}N_0Q\right)^{-1}V_0^{-1} \triangleq \mathcal{F}_\ell(J, Q),$$

where $Q \in \mathcal{RH}_\infty$ such that $(I + V_0^{-1}N_0Q)(\infty)$ is invertible and the generator system J can be implemented as

$$J = \begin{bmatrix} J_{11} & J_{12} \\ J_{21} & J_{22} \end{bmatrix} = \begin{bmatrix} \tilde{V}_0^{-1}\tilde{U}_0 & \tilde{V}_0^{-1} \\ V_0^{-1} & -V_0^{-1}N_0 \end{bmatrix}. \tag{16}$$

Proof. See the work of Zhou et al.[15] □

In words, by a Q-parameterization shown in Figure 2B, every linear internally stabilizing controller K can be implemented as a lower fractional transformation $K(Q) = \mathcal{F}_\ell(J, Q)$. That is, some central system J, where J_{11} is the nominal controller K_0, is interconnected with another stable filter $Q \in \mathcal{RH}_\infty$ such that

$$\text{col}(\boldsymbol{u}, \boldsymbol{r}) = [J]\text{col}(\boldsymbol{y}, \boldsymbol{s}), \quad \boldsymbol{s} = Q\boldsymbol{r}. \tag{17}$$

Note that the relationship between K and Q is bijective and that the nominal controller K_0 is recovered by $Q = 0$.

2.4.2 | Dual-Youla parameterization

The dual parameterization is most known for its use in closed-loop system identification in the Hansen scheme.[27] In addition, parameterizations of the dual form play a key role to reduce conservatism in the robust design of advanced motion control systems; see the work of Oomen.[28] The dual parameterization characterizes[8,22] in terms of a stable parameter system S all systems that are stabilized by one particular given controller.

Proposition 2 (S-parameterization). *Given coprime factorizations (12) of the nominal plant G and the controller K_0 that fulfill (13), the set of all proper plants stabilizable by K_0 is characterized in terms of an arbitrary stable operator S as $\mathcal{G} = \{G(S) \mid S \in \mathcal{S} \subseteq \mathcal{RH}_\infty\}$, where*

$$G(S) = N(S)M(S)^{-1}, \text{ with } N(S) = N_0 + V_0 S, \quad M(S) = M_0 + U_0 S, \text{ or} \tag{18}$$

$$G(S) = \tilde{M}(S)^{-1}\tilde{N}(S), \text{ with } \tilde{M}(S) = \tilde{M}_0 + S\tilde{U}_0, \quad \tilde{N}(S) = \tilde{N}_0 + S\tilde{V}_0. \tag{19}$$

Proof. The coprime factors of $G(S)$ and of K_0 satisfy the Bezout identity; hence, the result is dual to Proposition 1. A detailed derivation is spelled out in Chap. 3.4 in the work of Tay et al.[22] □

The relation between any S and the corresponding $G(S)$ is bijective, and the nominal system G_0 is recovered by $S = 0$. Note that $S \notin \mathcal{RH}_\infty$ implies that the pair $(G(S), K_0)$ is not stabilizing.

2.4.3 | Double-Youla parameterization

Combining the above parameterizations of plant $G(S)$ and controller $K(Q)$, the double-Youla parameterization[22] is obtained. It describes the set of loops formed by a nominal plant/controller interconnection and perturbations of the closed loop by systems S and Q.

Proposition 3 (Double-Youla parameterization). *Let (G_0, K_0) be a stabilizing nominal plant/controller pair, let $G(S)$ be the class of plants described by (18)-(19), and let $K(Q)$ be the class of controllers (14)-(15). Then, $(G(S), K(Q))$ is well-posed and internally stable if and only if the feedback system (Q, S) is well-posed and internally stable, ie, there exists*

$$\begin{bmatrix} I & -Q \\ -S & I \end{bmatrix}^{-1} \in \mathcal{RH}_\infty.$$

Proof. See Th. 2.1 in the work of Tay et al.[29] ☐

Let us emphasize in particular that the transfer function matrix from the input s to the output r in the *closed* loop of Figure 2B is the parameter S. Thus, to establish robust stability under both plant and controller uncertainty, the nominal plant/controller interconnection has to be stable, as well as the loop (Q, S). For a more detailed exposition, the reader is referred to the work of Tay et al.[22] Proposition 3 allows to characterize the set Q of maximally allowed perturbations $Q \in \mathcal{Q}$ of the controller K subject to robust stability of the closed loop for some set S of permissible models $S \in \mathcal{S}$.

Proposition 4 (Stable plant/controller perturbations). *Consider a set of plants $\mathcal{G}$ and a set of controllers $\mathcal{K}$ given by*

$$\mathcal{G}(G_0, K_0, \gamma_S) \triangleq \{(N_0 + V_0 S)(M_0 + U_0 S)^{-1} \mid \|S\|_\infty \leq \gamma_S\}, \quad \mathcal{K}(G_0, K_0, \gamma_Q) \triangleq \{(U_0 + M_0 Q)(V_0 + N_0 Q)^{-1} \mid \|Q\|_\infty \leq \gamma_Q\}.$$

Then, all plants in $\mathcal{G}$ are stabilized by all controllers in $\mathcal{K}$ if and only if $\gamma_S \cdot \gamma_Q < 1$.

Proof. This follows directly from application of the small-gain theorem[30] on the (Q, S) loop; see pp. 166f, 224 in the work of Tay et al.[22] ☐

Early investigations of such parameterizations were motivated by adaptive robust performance enhancement.[29] The advantages of the double-Youla framework are its inherent handling of uncertainty, the variety of design methods nowadays documented in the literature on the basis of the Youla parameter, and finally its nonconservatism compared to using other robustness metrics such as the Vinnicombe gap metric.[31] Therefore, recent work exploits the double parameterization approach, eg, to establish robust stability for systematic coupling controller design[32] or switching control for uncertain systems.[33] A double-Youla parameterization that is particularly suitable for implementation on robotic systems will be derived in Section 4.

2.5 | Robust AID control

Before we proceed to characterize robust AID controllers via the double-Youla parameterization, a brief overview of the related work is given. The robust control of robot manipulators has been subject to research for decades, and a wealth of methods have been developed,[1-4] based on a multitude of underlying approaches, eg, linear multivariable, passivity-based, sliding mode.[34,35] We therefore review selected work paradigmatically by ascending dynamic model demand.

Static and model free. It has long been known that a high-gain PD controller applied directly to the nonlinear rigid-body system robustly yields uniform ultimate boundedness of the tracking error.[36,37] Design methods for gain selection are nonetheless being investigated today[38] and a high-gain PD controller can be suitable even for fast dynamic manipulation tasks.[39]

Based on crude approximation. Even if not based on inverse dynamics, robust manipulator control methods typically employ a nominal inertia model, eg, using a disturbance observer[40] or model-free time delay control.[41] That is, only the most dominant part of the manipulator dynamics is approximated and the rest is treated as an uncertain disturbance input.[42-44] Taking only a diagonal estimate of the inertia matrix, the problem is handled as a linear decoupled system subject to the disturbances induced by neglected cross-coupling terms. This way, it is always possible to achieve $\alpha < 1$ in (9). In the authors' experience,[11] this approach constitutes a viable trade-off to build a parameterization-based robustly stable learning control system that noticeably exploits domain knowledge without a detailed dynamical model of the robot manipulator at hand.

Nonlinear model-based. Taking a nonlinear dynamical model of the robot manipulator allows to accomplish a better approximate feedback linearization. Nonetheless, the model (6) is always imprecise to a certain extent, ie, (7) and (8) do not vanish. Classic robust manipulator control methods[1-4] therefore design the outer-loop controller to ensure robust stability of the overall loop. Recent research also considers performance or optimality criteria, eg, $\mathcal{H}_\infty$ optimality,[45] time-domain bounds,[46] or orbital stabilization around the desired trajectory.[47]

Most relevant for the developments in this article are the classic linear multivariable design[9] and the Lyapunov-based robust manipulator control designs[5] reviewed in more detail next.

2.5.1 | The linear multivariable approach

A double-Youla parameterization allows to consider perturbations of both the controller and the plant models. The early robust manipulator control methods, in contrast, only exploit the characterization of all stabilizing compensators for the linear unperturbed model. Spong and Vidyasagar[9] were able to show that one can always find a linear control law stabilizing the nonlinear loop resulting from AID if the dynamic model of the robot satisfies Assumptions 1 and 2 and $\alpha < 1$ in (9). To this end, consider the control

$$\boldsymbol{u} = \ddot{\boldsymbol{q}}_{\mathrm{d}} + \boldsymbol{v}, \tag{20}$$

where the additional term $\boldsymbol{v}$ is supposed to increase the robustness against the uncertainties due to the approximate controller (3). Inserting (20) and (3) into (1), the resulting error dynamics read

$$\dot{\boldsymbol{e}} = \begin{bmatrix} \boldsymbol{0} & \boldsymbol{I} \\ \boldsymbol{0} & \boldsymbol{0} \end{bmatrix} \boldsymbol{e} + \begin{bmatrix} \boldsymbol{0} \\ \boldsymbol{I} \end{bmatrix} (\boldsymbol{\eta} + \boldsymbol{v}), \tag{21}$$

where the vector $\boldsymbol{\eta}$ is induced by the uncertainty resulting from the approximate model in the closed loop:

$$\boldsymbol{\eta} = \boldsymbol{\Delta}_{\mathrm{M}}(\ddot{\boldsymbol{q}}_{\mathrm{d}} + \boldsymbol{v}) + \boldsymbol{M}^{-1}(\widetilde{\boldsymbol{n}} + \boldsymbol{\tau}_{\mathrm{d}}). \tag{22}$$

Hence, $\boldsymbol{\eta}(\ddot{\boldsymbol{q}}_{\mathrm{d}}, \boldsymbol{q}, \dot{\boldsymbol{q}}, \boldsymbol{v})$ is a nonlinear term that cannot simply be rejected as if it were an external disturbance. Instead, under the assumptions (9) and (10) with $\alpha < 1$, it is shown in the work of Spong and Vidyasagar[9] that, for some constants b and δ, the bound $\|\boldsymbol{\eta}\|_{\mathcal{L}_{\mathrm{T}\infty}} \leq (\delta\beta_1 + \alpha\beta_3)\|\boldsymbol{\eta}\|_{\mathcal{L}_{\mathrm{T}\infty}} + b$ holds, where $\|\cdot\|_{\mathcal{L}_{\mathrm{T}\infty}}$ denotes the truncated $\mathcal{L}_\infty$ norm.[30] Then, if $(\delta\beta_1 + \alpha\beta_3) < 1$, the control $\boldsymbol{v}$, the tracking error $\boldsymbol{e}$, and the uncertainty $\boldsymbol{\eta}$ are bounded. A sequence of Youla parameters Q_k is thus designed such that $\beta_1 \to 0$ and $\beta_3 \to 1$ for $k \to \infty$. The resulting robust controller K_k is finally given from (15) and is generally a high-gain dynamic compensator.

2.5.2 | Lyapunov-based method

Another popular approach to design a robust control input $\boldsymbol{u}$ for (3) is based on Lyapunov's second method.[1-4] It is usually assumed that a PD controller with feedforward acceleration compensation and an additional input term $\boldsymbol{v}$ is employed in the outer loop,

$$\boldsymbol{u} = \ddot{\boldsymbol{q}}_{\mathrm{d}} + \boldsymbol{K}_{\mathrm{P}}(\boldsymbol{q}_{\mathrm{d}} - \boldsymbol{q}) + \boldsymbol{K}_{\mathrm{D}}(\dot{\boldsymbol{q}}_{\mathrm{d}} - \dot{\boldsymbol{q}}) + \boldsymbol{v}, \tag{23}$$

which results in the error system

$$\dot{\boldsymbol{e}} = \begin{bmatrix} \boldsymbol{0} & \boldsymbol{I} \\ -\boldsymbol{K}_{\mathrm{P}} & -\boldsymbol{K}_{\mathrm{D}} \end{bmatrix} \boldsymbol{e} + \begin{bmatrix} \boldsymbol{0} \\ \boldsymbol{I} \end{bmatrix} (\boldsymbol{\eta} + \boldsymbol{v}). \tag{24}$$

Similar to (21)-(22), the uncertainty in the closed loop is lumped in a single term $\boldsymbol{\eta}$ and one needs to select an appropriate control Lyapunov function to design $\boldsymbol{v}$ so as to suppress the destabilizing effects of $\boldsymbol{\eta}$. For the details and assumptions underlying the classic approach, the reader is referred to Chap. 6.5.3 of the work of Sciavicco and Siciliano,[2] the work of Spong et al,[3] and Chap. 5.2 of the work of Lewis et al.[4]

2.5.3 | Drawbacks of established approaches

The robot control methods based on the approaches of Sections 2.5.1 and 2.5.2 have a number of drawbacks in common. First, all of the AID uncertainty is lumped in a single quantity $\boldsymbol{\eta}$. However, it is clear from (6) that an inaccurate inertia model results in multiplicative input uncertainty, whereas the neglected manipulator nonlinearities induce the inverse additive disturbance $\boldsymbol{\psi}$. Therefore, the structure of (6) is dismissed when the analysis starts with a single term $\boldsymbol{\eta}$. Second, an outer-loop PD controller is commonly[1-4] applied to stabilize (6) *prior to the robustness analysis*. Therefore, in all subsequent developments, one has to work with an error system (24) where the gains $\boldsymbol{K}_{\mathrm{P}}, \boldsymbol{K}_{\mathrm{D}}$ of the controller occur in the dynamic matrix $\boldsymbol{A}$.

These aspects entail unfavorable consequences. The additional input $\boldsymbol{v}$ must be carefully constructed to suppress the internal nonlinear disturbance $\boldsymbol{\eta}$, and it remains prohibitive, in general, to adapt $\boldsymbol{v}$ on the fly by data-driven methods. Furthermore, to design $\boldsymbol{v}$, a scalar bound $\|\boldsymbol{\eta}\| \leq \rho(\|\boldsymbol{e}\|)$ is required, which in the classic robust manipulator control[1-4] depends on the gains $\|[\boldsymbol{K}_{\mathrm{P}}, \boldsymbol{K}_{\mathrm{D}}]\|$ of the nominal PD controller. Thus, as pointed out in the works of Bascetta and Rocco[5] and Abdallah et al,[34] higher gains in the controller require stronger robustifying inputs $\boldsymbol{v}$ to correct for *seemingly* higher

uncertainty. In contrast, the practitioner's approach of using a high-gain PD controller is widely known to work robustly in practice. For the Lyapunov-based design, this discrepancy has been resolved by Bascetta and Rocco in the revised design.[5] We will return to these works by comparing to our novel parameterization in Section 5.3.

3 | MAIN RESULT

Our main goal is to shape a set of admissible controller perturbations such that numerous advanced design methods are applicable for enhancement of the AID-based controllers in a strict robust stability framework. To circumvent the drawbacks summarized in Section 2.5.3, we keep the uncertainty separated throughout instead of lumping the effects of (7)-(8) into a single additive term. As a sideline, we derive bounds on the perturbations to (6) *before* any outer-loop controller comes into place. To eventually keep the influence of the outer-loop controller transparent as well, we describe the uncertainty by means of the dual-Youla parameter. Therefore, in the framework proposed next, by construction, the uncertainty due to AID remains clearly distinguishable from the gains of the outer-loop controller.

3.1 | Problem statement

It is unfortunately not obvious to find in the literature[1-4,26,48] a suitable generalized plant[15,49] description for AID, as most methods work with error dynamics (21) or (24). Therefore, the first problem we tackle is how the standard robotic bounds (9)-(10) translate into a generalized setup (Figure 3A) without lumping the effects of (7)-(8) into a single additive term.

Problem 1 (Generalized plant formulation of AID). Given the system (1) and the control law (3) with Assumptions 1 and 2 fulfilled, reformulate the AID (6) and the corresponding bounds as a system

$$G : \begin{cases} \boldsymbol{z}_\Delta = G_{z_\Delta w_\Delta} \boldsymbol{w}_\Delta + G_{z_\Delta w} \boldsymbol{w} + G_{z_\Delta u} \boldsymbol{u} \\ \boldsymbol{z} = G_{zw_\Delta} \boldsymbol{w}_\Delta + G_{zw} \boldsymbol{w} + G_{zu} \boldsymbol{u} \\ \boldsymbol{y} = G_{yw_\Delta} \boldsymbol{w}_\Delta + G_{yw} \boldsymbol{w}, \end{cases} \tag{25}$$

such that the uncertainty (7) and (8) acting on the nominal double integrator $\ddot{\boldsymbol{q}} = \boldsymbol{u}$ is described by a linear fractional transformation as shown in Figure 3A. That is, the uncertainty is captured by an unknown norm-bounded Δ operating on the signals $\boldsymbol{z}_\Delta$ to yield the input perturbation $\boldsymbol{w}_\Delta$,

$$\boldsymbol{w}_\Delta(t) = \Delta(\boldsymbol{x}(t), t)\boldsymbol{z}_\Delta(t), \quad \text{where } \exists \delta \ \forall t : \|\Delta(\boldsymbol{x}(t), t)\| \leq \delta. \tag{26}$$

In the next step, we analyze how these bounds affect the closed-loop system when the nominal outer-loop controller is applied.

Problem 2 (Dual-Youla bound of uncertainty under AID). Given the system (25)-(26) and a nominal outer-loop stabilizing controller K_0, characterize by means of a dual-Youla bound $\|S\|_\infty \leq \gamma_S$ the worst-case dynamic perturbation in closed-loop w.r.t. the nominal controlled plant $\ddot{\boldsymbol{q}} = \boldsymbol{u}$.

The main result is a parameterization of robustly stabilizing controllers for the rigid-body manipulator under AID control. Once Problem 2 is solved, the solution to the following problem is immediate.

Problem 3 (Double-Youla for robust approximate inverse dynamics). For a given robot under AID control as in Problems 1 and 2, characterize in terms of the parameter set Q a subset of robustly stabilizing controllers $\mathcal{K}_R \subset K(Q)$.
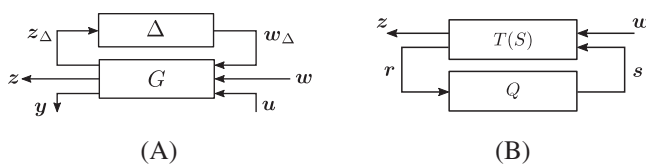

FIGURE 3 Open-loop uncertainty plant description Δ and double-Youla parameterization under external inputs. A, Generalized plant setup with uncertainty Δ in open loop; B, Reformulation as prestabilized uncertain closed loop $T(S)$ and controller parameterization via Q

3.2 | Generalized plant formulation of uncertainty bounds

We first tackle Problem 1 to obtain an uncertainty formulation in the form of the generalized plant depicted in Figure 3A. For convenience, let us restate (6) in the form

$$\ddot{\boldsymbol{q}} = \boldsymbol{u} + \boldsymbol{w}_{\Delta}^{\mathrm{U}} + \boldsymbol{w}_{\mathrm{dist}}, \tag{27}$$

where external disturbances $\boldsymbol{w}_{\mathrm{dist}} \triangleq \boldsymbol{M}^{-1}(\boldsymbol{q})\boldsymbol{\tau}_{\mathrm{dist}}$, and the vector of internal model uncertainty $\boldsymbol{w}_{\Delta}^{\mathrm{U}} = \boldsymbol{w}_{\Delta}^{\mathrm{M}} + \boldsymbol{w}_{\Delta}^{\psi}$ is summing up both inertia-induced uncertainty $\boldsymbol{w}_{\Delta}^{\mathrm{M}}$ and signal uncertainty $\boldsymbol{w}_{\Delta}^{\psi}$:

$$\boldsymbol{w}_{\Delta}^{\mathrm{M}} \triangleq \boldsymbol{\Delta}_{\mathrm{M}}(\boldsymbol{q}, \hat{\boldsymbol{q}})\boldsymbol{u}, \qquad \boldsymbol{w}_{\Delta}^{\psi} \triangleq \boldsymbol{M}^{-1}(\boldsymbol{q})\widetilde{\boldsymbol{n}}(\boldsymbol{q}, \dot{\boldsymbol{q}}, \hat{\boldsymbol{q}}, \hat{\dot{\boldsymbol{q}}}).$$

Subsequently, the dependency on joint positions and velocities is dropped for brevity in notation. With Assumption 3 the summand $\boldsymbol{w}_{\mathrm{dist}}$ is bounded by $\|\boldsymbol{w}_{\mathrm{dist}}\|_{\mathcal{L}_{\infty}} \leqslant M_{\mathrm{u}} C_{\mathrm{dist}}$ and depending neither on state nor on control; $\boldsymbol{w}_{\mathrm{dist}}$ is therefore considered as external disturbance input. Note that by (9)-(10), both $\boldsymbol{w}_{\Delta}^{\mathrm{M}}$ and $\boldsymbol{w}_{\Delta}^{\psi}$ are nondynamic, time-varying nonlinear uncertainties; it is therefore possible to use a norm-bounded uncertainty description (26), where the upper bound on the induced matrix norm $\|\Delta\| \triangleq \max_{\boldsymbol{z}_{\Delta}(t) \neq 0} \frac{\|\Delta \boldsymbol{z}_{\Delta}(t)\|}{\|\boldsymbol{z}_{\Delta}(t)\|} \leq \delta$ is satisfied for all times t (Sec. 2.3.1 in the work of Petersen and Tempo[50]). This corresponds to the maximum amplification over all input directions $\boldsymbol{z}_{\Delta}$ and is key to solving Problem 1.

Theorem 1 (Structured uncertainty under AID). *Under the conditions of Problem 1, the perturbed double integrator system (6) can be conservatively reformulated as a $G - \Delta$ structure depicted in Figure 4, where $\boldsymbol{w}_{\Delta} \triangleq col(\boldsymbol{w}_{\Delta}^{\mathrm{M}}, \boldsymbol{w}_{\Delta}^{\psi})$, $\boldsymbol{z}_{\Delta} \triangleq col(\boldsymbol{u}, z_{\Delta}^{\mathrm{f}}\boldsymbol{q}, \dot{\boldsymbol{q}})$, $z_{\Delta}^{\mathrm{f}} \equiv 1$ and $\Delta(t) \in \mathcal{D}_{\Delta}$ with the perturbation set*

$$\mathcal{D}_{\Delta} = \left\{ \Delta = \begin{bmatrix} \boldsymbol{\Delta}_{\mathrm{M}} & \boldsymbol{0} \\ \boldsymbol{0} & \boldsymbol{\Delta}_{\Psi} \end{bmatrix} : \boldsymbol{\Delta}_{\mathrm{M}} \in \mathbb{R}^{n \times n}, \boldsymbol{\Delta}_{\Psi} \in \mathbb{R}^{n \times (2n+1)}, \|\boldsymbol{\Delta}_{\mathrm{M}}\| \leq \alpha_{\mathrm{M}}, \|\boldsymbol{\Delta}_{\Psi}\| \leq \alpha_{\Psi} \right\}. \tag{28}$$

The bounds α_M and α_Ψ are scalars given by (B3).

Proof. The derivation is given in Appendix B.1. $\qquad \square$

Remark 1 (Uncertainty separation). To obtain such a description, one could also work with $\boldsymbol{w}_{\Delta}^{\mathrm{U}} = \Delta^{\mathrm{U}}\boldsymbol{z}_{\Delta}$ instead of collecting the terms $\boldsymbol{w}_{\Delta}^{\mathrm{M}}$, $\boldsymbol{w}_{\Delta}^{\psi}$ of (27) separately in the vector $\boldsymbol{w}_{\Delta}$. Then, however, the result is unstructured with an overly conservative bound on the uncertainty matrix Δ.

By adopting the uncertainty structure (28), the separation of the two uncertainty sources is preserved because the summation of $\boldsymbol{u}$, $\boldsymbol{w}_{\Delta}^{\mathrm{M}}$, and $\boldsymbol{w}_{\Delta}^{\psi}$ in (27) is captured by the signal interconnection in the generalized plant G, as depicted in Figure 4. Therefore, this structure is carried into the dual-Youla operator in the sequel.

3.3 | Dual-Youla uncertainty characterization

We now calculate a realization of the uncertain dual-Youla parameter S when the nominal controller K_0 is applied to stabilize the uncertain plant $\mathcal{F}_u(G, \Delta)$. Recall that in (18)-(19) all systems stabilized by K_0 are parameterized as $\mathcal{G}$.
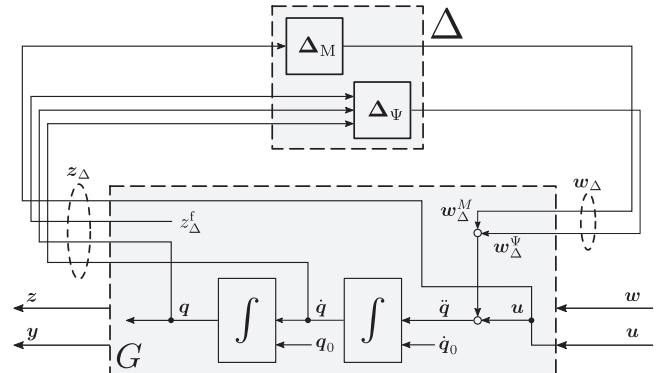
FIGURE 4 Generalized plant interconnection of a robot manipulator under approximate inverse dynamics control with uncertainties "pulled out."[15] This figure only depicts the perturbed double integrator system and the uncertainty, ie, the G-Δ structure suitable for subsequent analyses. The precise configuration of the control and performance channels $\boldsymbol{y}, \boldsymbol{z}$ depends on the manipulator control goal at hand, eg, tracking or impedance control. A tracking control example is given in Section 5 with the corresponding state-space realization in Appendix C

Consequently, if $G_{yu}(\Delta) = \mathcal{F}_u(G, \Delta)$ is robustly stabilized by K_0, ie, $G_{yu}(\Delta) \in \mathcal{G}$ for all $\Delta \in \mathcal{D}_\Delta$, then equivalently there exists an uncertain $S \in \mathcal{S}_\Delta \subseteq S$. Key to our approach is the following explicit connection of the open-loop uncertainty description in terms of Δ and in terms of the S obtained in the closed loop with K_0 applied (Th. 3.4 in the work of Niemann,[12] and the work of Niemann and Stoustrup[51]):

$$G_{yu}(S) = G_{yu}(\Delta) \quad \Leftrightarrow \quad S(\Delta) = T_{\Delta,21}\Delta(I - T_{\Delta,11}\Delta)^{-1}T_{\Delta,12} = \mathcal{F}_u(T_\Delta, \Delta). \tag{29}$$

In (29), T_Δ refers to the mapping from the inputs $\mathrm{col}(\boldsymbol{w}_\Delta, \boldsymbol{s})$ to the outputs $\mathrm{col}(\boldsymbol{z}_\Delta, \boldsymbol{r})$. In operator notation, T_Δ is expressed as

$$T_\Delta = \begin{bmatrix} G_{z_\Delta w_\Delta} + G_{z_\Delta u}U_0\tilde{M}_0 G_{yw_\Delta} & G_{z_\Delta u}M_0 \\ \tilde{M}_0 G_{yw_\Delta} & 0 \end{bmatrix}. \tag{30}$$

Remark 2. As Niemann[12] points out, "S depends only on the uncertain block Δ and the coprime factors." For the purpose of this paper, however, we would like to emphasize the fact that (29) and (30) also depend on the interconnection used in the generalized plant (25). This is an important feature of this article: in contrast to the robust control approaches summarized in Section 2.5, by the derivation in Section 3.2, we keep the inertia-induced uncertainty $\boldsymbol{w}_\Delta^M$ completely separated from the nonlinear inputs $\boldsymbol{w}_\Delta^\psi$, thus reducing the conservatism of the resulting S.

With the generalized plant of Figure 4 and the bounded perturbation set $\mathcal{D}_\Delta$ from (28), we obtain the following result.

Theorem 2 (Realization of dual-Youla uncertainty set). *Consider the system (1) with the AID controller (3) such that Assumptions 1 and 2 are fulfilled. According to Section 3.2, the resulting system dynamics is conservatively covered by the linear, stabilizable, and detectable plant (25) with a state-space realization (C1) and the uncertainty structure (28). Let a nominal linear controller*

$$K_0 \triangleq \left[\begin{array}{c|c} A_K & B_K \\ \hline C_K & D_K \end{array} \right] \tag{31}$$

be applied to the outer loop, with the pairs (A_K, B_K) stabilizable and (A_K, C_K) detectable. Let the state-feedback gains F_G and F_K be designed such that $A_{11} + B_{13}F_G$ and $A_K + B_KF_K$ are stable. Then, the set of uncertain dual-Youla operators is given by

$$S_\Delta = \left\{ S(\Delta) : \left[\begin{array}{c|c} A_S & B_S \\ \hline C_S & D_S \end{array} \right], \ \forall \Delta \in \mathcal{D}_\Delta \right\}, \tag{32}$$

where

$$A_S = \begin{bmatrix} B_{13}D_KC_{31} + A_{11} & B_{13}C_K & A_{S,13} & A_{S,14} \\ B_KC_{31} & A_K & B_KD_{31}\Delta\bar{C} & A_{S,24} \\ 0 & 0 & \bar{A} & \bar{B}C_{11} + \bar{B}D_{13}F_G \\ 0 & 0 & 0 & B_{13}F_G + A_{11} \end{bmatrix}, \quad B_S = \begin{bmatrix} B_{S,11} \\ B_KD_{31}\Delta\bar{D}D_{13} \\ \bar{B}D_{13} \\ B_{13} \end{bmatrix}, \tag{33}$$

$$C_S = \begin{bmatrix} C_{31} & -F_K & D_{31}\Delta\bar{C} & D_{31}\Delta\bar{D}C_{11} + D_{31}\Delta\bar{D}D_{13}F_G \end{bmatrix}, \quad D_S = D_{31}\Delta\bar{D}D_{13},$$

$$A_{S,13} = B_{11}\Delta\bar{C} + B_{13}D_KD_{31}\Delta\bar{C},$$

$$A_{S,14} = B_{11}\Delta\bar{D}C_{11} + B_{11}\Delta\bar{D}D_{13}F_G + B_{13}D_KD_{31}\Delta\bar{D}C_{11} + B_{13}D_KD_{31}\Delta\bar{D}D_{13}F_G,$$

$$A_{S,24} = B_KD_{31}\Delta\bar{D}C_{11} + B_KD_{31}\Delta\bar{D}D_{13}F_G, \quad B_{S,11} = B_{11}\Delta\bar{D}D_{13} + B_{13}D_KD_{31}\Delta\bar{D}D_{13},$$

and the expressions for $\bar{A}, \bar{B}, \bar{C}, \bar{D}$ are given by the realization (B6).

Proof. The proof is given in Appendix B.2. $\square$

From the realization (33), it becomes apparent that S is much more involved than the diagonal uncertainty structure of Δ. Hence, standard robustness tools[52] such as μ analysis[53] or worst-case gain assessment[54] cannot be directly applied.

To solve Problem 2, it is nonetheless required to find an estimate $\hat{\gamma}_S$ of the worst-case gain

$$\gamma_S \triangleq \sup_{S \in \mathcal{S}_\Delta} \|S\|_\infty. \tag{34}$$

To this end, we propose to adopt a randomized approach[55] allowing for the following probabilistic worst-case assessment.

Proposition 5 (Probabilistic dual-Youla uncertainty bound). *Assign with $p \in (0,1), \delta \in (0,1)$ the desired probability level such that $P(\|S(\Delta)\|_\infty \leq \hat{\gamma}_S) \geq p, \ \forall \Delta \in \mathcal{D}_\Delta$ holds with probability $1-\delta$. The corresponding gain bound $\hat{\gamma}_S$ is obtained by the empirical maximum $\hat{\gamma}_S = \max_{i=1, \ldots, n_S} \|S_i\|_\infty$, using $n_S \geq \left\lceil \frac{\ln 1/\delta}{\ln 1/p} \right\rceil$ iid samples from $\mathcal{D}_\Delta$.*

Proof. This follows directly from the definition of probabilistic worst-case performance assessment using a randomized algorithm.[55] □

A procedure to obtain $\hat{\gamma}_S$ correspondingly is summarized in Algorithm 1.

Algorithm 1 Calculation of worst-case gain estimate $\hat{\gamma}_S$

Input: p, δ – desired probability levels $\qquad\qquad\qquad$ α_M, α_Ψ – norm bounds (B3)
$\qquad$ G – realization (C1) of G, eg, according to Appendix C $\qquad$ K_0 – realization of nominal controller
$\qquad$ F_G – stabilizing state feedback for plant $\qquad\qquad\qquad$ F_K – stabilizing state feedback for controller

1: $n_S \leftarrow \text{ceil}\left(\ln\frac{1}{\delta} \big/ \ln\frac{1}{p}\right)$
2: **for** $i = 1, 2, 3, \ldots, n_S$ **do**
3: $\qquad \Delta_i^M \leftarrow$ draw sample uniformly over $\mathcal{B}_2^{n \times n}(\alpha_M), \qquad \Delta_i^\Psi \leftarrow$ draw sample uniformly over $\mathcal{B}_2^{n \times (2n+1)}(\alpha_\Psi)$
4: $\qquad S_i \leftarrow S\left(\text{blkdiag}\left(\Delta_i^M, \Delta_i^\Psi\right)\right)$ by (33)
5: **end for**
6: $\hat{\gamma}_S \leftarrow \max_{i=1,\ldots,n_S} \|S_i\|_\infty$

Output: $\hat{\gamma}_S$

Remark 3 (Realization of dual-Youla parameter for norm-bounded memoryless uncertainty). The state-space realization for the dual-Youla parameter S according to (33) is a fairly general result by itself: It covers, under the usual assumptions for double-Youla parameterizations, the linear generalized plant interconnection of the form (C1) subject to nondynamic (memoryless) norm-bounded uncertainty Δ, while allowing for any linear central controller K_0 in the Q-parameterization. Thus, the result extends[12] in that, due to the symbolic derivation, the realization of S given in (33) is explicit in the state-space matrices and hence suitable for numeric computation of the $\mathcal{H}_\infty$-norm. By contrast, in our simulation study reported in Section 5, a straightforward* implementation by (29) quickly becomes inaccurate, presumably because of the numeric inversion that easily yields badly conditioned systems.

3.4 | Characterization of robustly stabilizing controllers

With S according to (29) and (33), respectively, the control loop can now be described as shown in Figure 3B. The loop $T(S)$ is stabilized but uncertain and the controller is determined by some $Q \in \mathcal{Q}$. Writing out the matrix transfer operator $T_{zw}(S, Q) = \mathcal{F}_\ell(T(S), Q)$ from references $\mathbf{w}$ to outputs $\mathbf{z}$, one obtains

$$T_{zw}(S, Q) = T_{11}(S) + T_{12}(S)Q(I - T_{22}(S)Q)^{-1}T_{21}(S).$$

The following sufficient condition is established to ensure the overall stability of the scheme.

---
*Direct computation of S by formula (29) using MATLAB state-space objects `ss` yields `hinfnorm(S,1e-6)=inf` although S is stable.

Lemma 1 (Double Youla under exogenous disturbance and plant uncertainty). *Under the previous assumptions, for all $\Delta \in \mathcal{D}_\Delta$, there exists correspondingly an $S \in \mathcal{S}_\Delta$. Denote by $\mathcal{Q}$ the set of finite-gain stable, admissible parameters $Q \in \mathcal{Q}$. Referring to Figure 3, $T_{zw}(S, Q)$ is robustly stable if both of the following conditions hold.*

(i) K_0 robustly stabilizes the uncertain plant $\mathcal{F}_u(G, \Delta)$, ie,

$$\forall \Delta \in \mathcal{D}_\Delta \ : \ \begin{bmatrix} I & -\begin{bmatrix} 0 & 0 \\ 0 & K_0 \end{bmatrix} \\ -\mathcal{F}_u(G, \Delta) & I \end{bmatrix}^{-1} \in \mathcal{RH}_\infty, \tag{35}$$

(ii) the loop (Q, S) is stable and $\forall Q \in \mathcal{Q}, \forall S \in \mathcal{S}_\Delta$: $\quad \|Q\|_\infty \|S\|_\infty < 1$.

Proof. Please refer to Appendix B.3. $\qquad \square$

By the condition (ii), it is immediate to characterize a set of controller parameters $\mathcal{Q}$ that preserves robust stability and is suitable for a wide range of performance enhancement methods.

Theorem 3 (Set of robust AID controllers). *Under the assumptions of Theorem 2, let the worst-case gain (34) be estimated by $\hat{\gamma}_S \xrightarrow{\geqslant} \gamma_S$. If $\hat{\gamma}_S$ is finite, K_0 is robustly stabilizing. A subset of all robustly stabilizing controllers is then given by*

$$\mathcal{K}_R = \{K(Q) : (14) - (15) \text{ and } \|Q\|_\infty < 1/\hat{\gamma}_S\}, \tag{36}$$

and every controller $K \in \mathcal{K}_R$ stabilizes the nonlinear system (6)-(8).

Proof. According to Theorem 1, the uncertain nonlinear dynamics (6)-(8) are conservatively covered by the uncertainty structure $\mathcal{D}_\Delta$ from (28). As by Theorem 2, $\mathcal{D}_\Delta$ corresponds to $\mathcal{S}_\Delta$ when the nominal controller K_0 is applied. With Proposition 5, $\hat{\gamma}_S$ is the worst-case gain over all $\mathcal{S}_\Delta$ by letting $p \to 1, \delta \to 0$. The result is then a direct consequence of Lemma 1. $\qquad \square$

On the one hand, the first condition (i) of Lemma 1, ie, robust stability of the uncertain loop with only the nominal controller applied, may seem quite restrictive. On the other hand, the stability of the (Q, S) loop is ensured by a small-gain argument; thus, it also guarantees internal stability when Q is a nonlinear or time-varying stable operator with an appropriately defined stability notion.[30] Hence, due to the double-Youla parameterization, a variety of advanced methods can be used for manipulator control design in the proposed rigorous robust stability framework (cf Figure 1).

Remark 4 (Model complexity trade-off). Theorem 3 provides a way to *quantify* the trade-off between the accuracy of the available manipulator model and the amount of controller enhancement permissible without sacrificing robust stability of the system: A very imprecise robot model will yield large γ_S and consequently $\mathcal{K}_R \to \{K_0\}$ as $\mathcal{Q} \to \emptyset$. As for the other extreme, a perfect model allows for a true feedback linearization; hence, $S = 0$, and by $\hat{\gamma}_S \to 0$, Theorem 3 recovers the set of all controllers that stabilize a double integrator.

Remark 5 (Robust stability under nominal control). If the nominal controller K_0 does not stabilize the system under all perturbations $\Delta \in \mathcal{D}_\Delta$, then $\gamma_S = \infty$, ie, there is some unstable $S(\Delta)$. In such cases, it may via Q still be possible to adaptively stabilize the (Q, S) loop of the double-Youla parameterization.[29] We do not pursue such approaches further but restrict attention to a more robust setting: here, stabilization under all perturbations $\Delta \in \mathcal{D}_\Delta$ by means of all controllers (36) is the asset allowing for straightforward online performance enhancement.

4 | SPECIAL CASE: STATIC NOMINAL CONTROL

In this section, we specialize the main result to the very commonly used controller of the PD-type (5) or (23) as initial controller K_0. To this end, under the previous assumptions, a Q-parameterization can be constructed as follows.

Proposition 6 (Central J for static nominal control[11]). *A realization of the central system J to build a Q-parameterization around a static controller for the system (C1) is*

$$J : \left[\begin{array}{cc|cc} A_{11} + B_{13}F_{\mathrm{G}} & \mathbf{0} & B_{13} \\ F_{\mathrm{G}} - D_0C_{31} & D_0 & I \\ -C_{31} & I & \mathbf{0} \end{array}\right], \quad x_{\mathrm{J}}(0) = \mathbf{0}. \tag{37}$$

Proof. See the work of Friedrich and Buss.[11] □

A block diagram of (37) is depicted in Figure 5.

Remark 6 (Components of control input). Comparing to Section 2.5, the overall control signal corresponds exactly to the standard ansatz for the outer loop (23), but the additional signal δu is generated differently from the "robust-control term"[5] v, precisely model based in the Q-parameterization generated from (37).

Note that the central system J inherits with (37) a separation structure that is very useful for implementation on hardware: The two-port system (37) is given directly by the static nominal controller D_0 and some dynamic augmentation to generate the signal r. Referring to Figure 5, the augmentation J can be further simplified by choosing the coprime factor stabilizing gain F_{G} as

$$F_{\mathrm{G}} = D_0C_{31}. \tag{38}$$

By this choice, only the filtered output s is added to the control input $u = u_{\mathrm{nom}} + \delta u_{\mathrm{a}} + s \overset{(37)\,\text{with}\,(38)}{=} u_{\mathrm{nom}} + s$. Thus, the proposed special case is particularly simple to implement: Opposed to the standard Youla parameterization,[15] no observer-based central controller is required. Instead, robot manipulators that are already driven by a PD controller can be augmented to generate the parameterization.

To quantify the uncertainty in the closed loop by $\hat{\gamma}_{\mathrm{S}}$, an expression for the corresponding dual-Youla parameter is derived as well.

Corollary 1. *The realization of the uncertain dual-Youla parameter $S(\Delta)$ describing the AID effect (25), (28) controlled by (37) is given as*

$$S : \left[\begin{array}{ccc|c} A_{\mathrm{S},11} & A_{\mathrm{S},12} & A_{\mathrm{S},13} & B_{\mathrm{S},11} \\ \mathbf{0} & \bar{A} & \bar{B}C_{11} + \bar{B}D_{13}F_{\mathrm{G}} & \bar{B}D_{13} \\ \mathbf{0} & \mathbf{0} & A_{11} + B_{13}F_{\mathrm{G}} & B_{13} \\ \hline C_{31} & D_{31}\Delta\bar{C} & C_{\mathrm{S},13} & D_{31}\Delta\bar{D}D_{13} \end{array}\right], \tag{39}$$

where

$$A_{\mathrm{S},11} = B_{13}D_0C_{31} + A_{11}, \qquad A_{\mathrm{S},12} = B_{11}\Delta\bar{C} + B_{13}D_0D_{31}\Delta\bar{C},$$

$$A_{\mathrm{S},13} = B_{11}\Delta\bar{D}C_{11} + B_{11}\Delta\bar{D}D_{13}F_{\mathrm{G}} + B_{13}D_0D_{31}\Delta\bar{D}C_{11} + B_{13}D_0D_{31}\Delta\bar{D}D_{13}F_{\mathrm{G}},$$

$$B_{\mathrm{S},11} = B_{11}\Delta\bar{D}D_{13} + B_{13}D_0D_{31}\Delta\bar{D}D_{13}, \qquad C_{\mathrm{S},13} = D_{31}\Delta\bar{D}C_{11} + D_{31}\Delta\bar{D}D_{13}F_{\mathrm{G}},$$

$$\bar{A} = B_{11}\Delta\tilde{D}^{-1}C_{11} + B_{11}\Delta\tilde{D}^{-1}D_{13}D_0C_{31} + B_{13}D_0C_{31} + \tilde{B}C_{11} + \tilde{B}D_{13}D_0C_{31} + A_{11},$$

$$\bar{B} = -B_{11}\Delta\tilde{D}^{-1} - \tilde{B}, \qquad \bar{C} = -\tilde{D}^{-1}C_{11} - \tilde{D}^{-1}D_{13}D_0C_{31}, \qquad \bar{D} = \tilde{D}^{-1},$$

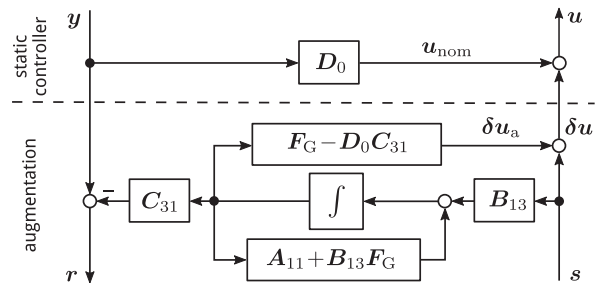$$\tilde{B} = B_{13}D_0D_{31}\Delta\tilde{D}^{-1}, \qquad \tilde{D} = I - D_{11}\Delta - D_{13}D_0D_{31}\Delta.$$

FIGURE 5 Central system J to generate a Q-parameterization, based on a static nominal controller $K_0 \triangleq D_0$. Note that the augmentation simplifies further by choosing $F_{\mathrm{G}} = D_0C_{31}$. In this case, $\delta u_{\mathrm{a}} = \mathbf{0}$ and consequently $u = u_{\mathrm{nom}} + s$

Proof. The derivation is analogous to the full case of Theorem 2, replacing the coprime factors with those for a static controller.[11] Alternatively, the given realization of S can be obtained from (33) by appropriately removing obsolete rows and columns for undefined A_K, B_K, C_K, and taking $D_K = D_0$. □

4.1 | Summary of the proposed robust manipulator control framework

The steps to employ the control design in practice are summarized as follows.

① Design a static nominal controller K_0 with the goal of ensuring robust stability to the uncertain system, given an underlying AID controller.
② Determine, eg, by simulation or experiment, an estimate of the norm bounds of Assumption 2 and 3 for the robot manipulator at hand and the bounds (9) and (10) that characterize the accuracy of the inverse dynamics controller.
③ Calculate by (B3) the bounds α_M and α_Ψ, corresponding to inertia respectively nonlinear signal uncertainty.
④ Obtain by Algorithm 1 an estimate $\hat{\gamma}_S$ of the worst-case dual-Youla operator norm.
⑤ Add the dynamic augmentation to build the central system (37) shown in Figure 5. Then, improve the performance by adding Q, designed by any suitable method, subject to $\|Q\|_\infty < 1/\hat{\gamma}_S$.

Steps ① and ② are standard, whereas steps ③–⑤ exploit the novel parameterization based on the double-Youla approach.

5 | DISCUSSION AND ILLUSTRATIVE STUDY

First, let us discuss the implications of the main result by the familiar planar elbow manipulator example. Next, the practical utilization of the proposed framework is illustrated by means of a robotic manipulator with six rotational DoFs under varying payload. We will finally compare the novel robust stability framework to the existing ones and outline how a variety of control design methods can be used in the control approach put forward in this article.

5.1 | Discussion of worst-case dual-Youla uncertainty measure

The dual-Youla characterization according to Proposition 5 of our main result provides a new perspective to uncertainty quantification in AID manipulator control.

5.1.1 | Example setup

As in the reference book,[4] we use a planar elbow manipulator with two rotational DoFs to illustrate the control scheme and discuss our results. For the description and detailed physical parameters of the particular manipulator, the reader is referred to the work of Schill and Buss.[39] The resulting model is given by (all in SI units)

$$\boldsymbol{M} = \begin{bmatrix} 0.162\cos(q_2) + 0.655 & 0.0809\cos(q_2) + 0.142 \\ 0.0809\cos(q_2) + 0.142 & 0.356 \end{bmatrix}, \quad \boldsymbol{C} = \begin{bmatrix} -0.0809\dot{q}_2\sin(q_2) & -0.0809\sin(q_2)(\dot{q}_1 + \dot{q}_2) \\ 0.0809 q_1 \sin(q_2) & 0 \end{bmatrix}, \quad (40a)$$

$$\boldsymbol{g} = \begin{bmatrix} 3.60\cos(q_1 + q_2) + 9.35\cos(q_1) \\ 3.60\cos(q_1 + q_2) \end{bmatrix}, \quad \boldsymbol{f} = \mathrm{blkdiag}(3.00, 3.00)\dot{\boldsymbol{q}}. \quad (40b)$$

A preliminary analysis yields the following numeric values of the bounds (A1) for this manipulator:

$$M_u = 3.765, \quad F_u = 3, \quad C_u = 1.289, \quad g_u = 13.44. \quad (41)$$

To analyze the interplay of the available model knowledge and the outer-loop controller w.r.t. the uncertainty $S(\Delta)$, the most commonly used controllers of type (3) are summarized in Table C1; the abbreviations PFL, AID, SID, DS, GC, and NID correspondingly refer to the inner-loop controllers in the following. The parameters used in the simulation study and the achievable uncertainty bounds are also given in Table C1.

Remark 7 (Two-DoF control). We employ a two-DoF control scheme in the sequel, ie, the feedforward and feedback gains can be tuned independently. By selecting $\boldsymbol{y} = \mathrm{col}(\hat{\boldsymbol{q}}, \dot{\hat{\boldsymbol{q}}}, \boldsymbol{q}_d, \dot{\boldsymbol{q}}_d, \ddot{\boldsymbol{q}}_d)$ instead of $\boldsymbol{y} = \mathrm{col}(\boldsymbol{e}, \dot{\boldsymbol{e}}, \ddot{\boldsymbol{q}}_d)$, the following developments hold for the general class of two-DoF controllers. We use the state-space realization as given by (C1)–(C2) in Appendix C, corresponding to a tracking control configuration of Figure 4.

To keep the following discussion simple, we restrict most of our attention to the specialization of the main result from Section 4. The central controller is based on static $\boldsymbol{u}_0 = K_0 \boldsymbol{y}$ with

$$K_0: \quad \boldsymbol{D}_0 = [-\boldsymbol{K}_p, -\boldsymbol{K}_d, \boldsymbol{K}_p, \boldsymbol{K}_d, \boldsymbol{K}_{ff}], \tag{42}$$

and the Q-parameterization is generated from (37). Consequently, S is calculated according to Corollary 1 unless stated otherwise. The stabilizing gains $\boldsymbol{F}_G, \boldsymbol{F}_K$ are design parameters in the construction of the stabilizing factorization (B4) of the plant and controllers and affect γ_S. In this section, no $\boldsymbol{F}_K$ is needed because of the static nominal controller, and unless stated differently, $\boldsymbol{F}_G$ is calculated by (38). Note that, by construction, S is a dynamical operator mapping $\boldsymbol{s} \in \mathbb{R}^{n_u}$ to $\boldsymbol{r} \in \mathbb{R}^{n_y}$; hence, in this example with two joints and $n_y = 10$ measurements according to Remark 7, S is a 10×2 uncertain system. With γ_S from (34) describing the worst-case uncertainty in the closed-loop system given a specific outer-loop controller, the following qualitative properties should be captured.

- Larger model uncertainty (ie, larger values of α_M, α_Ψ) should result in larger γ_S.
- Robust and high-gain nominal controllers should lead to lower γ_S.
- Feedforward control action should *not* increase uncertainty γ_S of the feedback loop.

By inspection of (33), all these aspects influence the expression for $S(\Delta)$; therefore, each will be discussed separately. To obtain $\hat{\gamma}_S$, the procedure from Table 1 is used with the confidence level set to $p = 99.99\%$ and $\delta = 10^{-4}$, corresponding to $n_S \geq 92099$ samples[†] over the uncertainty set $\mathcal{D}_\Delta$ for each calculation of $\hat{\gamma}_S$. A single evaluation of $\hat{\gamma}_S$ with 10^5 samples takes approximately 20 min on a current desktop computer (3.9 GHz, 32 GB of RAM) using MATLAB R2017a.

Remark 8 (Signal uncertainty for revolute manipulators). The example manipulator consists only of revolute joints; thus, a constant bound on the gravity error can be assumed. In other words, it is known *exactly* that $\|\widetilde{\boldsymbol{n}}\|$ does not depend on joint positions and consequently, the uncertainty on nonlinearities can be taken as a matrix $\boldsymbol{\Delta}_\Psi \in \mathbb{R}^{n \times (n+1)}$.

5.1.2 | Influence of AID parameters

We first investigate how the accuracy of the approximate model influences the worst-case gain γ_S. To this end, for now, assume that the outer-loop controller is a PD feedback controller for critical damping in the nominal loop, ie, it is defined by (42) with

$$\boldsymbol{K}_p = \mathrm{diag}(K_p, K_p), \boldsymbol{K}_d = \mathrm{diag}(K_d, K_d), \text{ where } K_p = 10^3, K_d = 63.3, \text{ and } \boldsymbol{K}_{ff} = \boldsymbol{0}. \tag{43}$$

First, consider the PFL case of Table C1, ie, $\alpha_M = \alpha_\Psi = 0$. Clearly, in this case, there is no uncertainty as the underlying feedback linearization uses a perfect model of the manipulator dynamics. The uncertainty set consequently degenerates to $\mathcal{D}_\Delta = \{\boldsymbol{0}\}$ and from (33) immediately $S = 0$ follows. As expected from Remark 4, the nominal decoupled double integrators describe the resulting loop perfectly.

In the robust control approaches reviewed in Section 2.5, the accuracy of the inertia model plays a crucial role as measured by the value of α from (9): Both Spong and Vidyasagar[9] and Bascetta and Rocco[5] need $\alpha < 1$ as a prerequisite. We therefore begin by investigating the influence of α_M on the worst-case gain γ_S while $\alpha_\Psi = 0$. The calculations were carried out over a fine grid on $0 < \alpha_M \leq 1.1$. The results are shown in Figure 6A. The uncertainty characterized by the worst-case $\|S(\Delta)\|_\infty$ is very low for $0 < \alpha_M < 0.7$. We can then observe a rapid increase for $0.7 < \alpha_M < 0.85$ and $\hat{\gamma}_S = \infty$, ie, unstable S, for values greater than $\alpha_M \approx 0.85$. In other words, robust stability of the inner AID loop using the PD controller with the gains (43) is lost for inertia uncertainty greater in norm than 0.85, given that $\widetilde{\boldsymbol{n}} = 0$.

Similarly, the influence of the norm of the neglected nonlinearities $\widetilde{\boldsymbol{n}}$ can be evaluated. To this end, we have calculated $\hat{\gamma}_S$ over a grid of $0 < \alpha_\Psi \leq 110$ with $\alpha_M = 0$. As depicted in Figure 6B, for low values of $0 \leq \alpha_\Psi < 50$, $\hat{\gamma}_S$ stays small with a sudden increase up to instability of S for $\alpha_\Psi > 63$. Comparing with Table C1, we find that, for the gains (43), robust stability cannot be concluded for the inner-loop controller types NID, GC, DS, and SID, while viable robustness is obtained under the AID law.

We also performed a parameter sweep calculation over a grid of both α_M and α_Ψ, as shown in Figure 7. It can be observed that there is a relatively clear boundary between model accuracy that allows for robust controller enhancement and too inaccurate modeling that results in $\hat{\gamma}_S = \infty$. Note that these values are depending on the controller gains and were obtained

---

[†]Implementations of suitable methods[55] for uniform sampling over norm-bounded real matrices are readily available.[56]
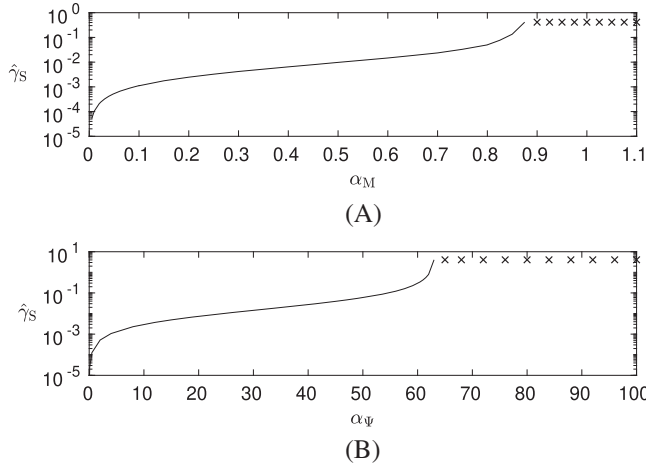
FIGURE 6 Influence of accuracy of inertia and nonlinearities' bounds on $\hat{\gamma}_S$. Unstable S are marked by x in the graphs only for visibility; by definition, $\gamma_S = \infty$ if S is not stable. A, Evaluation of $\hat{\gamma}_S$ using a fine discretization over the range of $0 < \alpha_M \leq 1.1$ and $\alpha_\Psi = 0$. A logarithmic scaling is used on the y-axis to visualize the change of $\hat{\gamma}_S$ in the order of magnitudes for $\alpha_M < 0.85$, up to instability of S occuring rapidly for $\alpha_M > 0.85$; B, Evaluation of the influence of α_Ψ with $\alpha_M = 0$. A logarithmic scaling is used on the y-axis for enhanced visibility
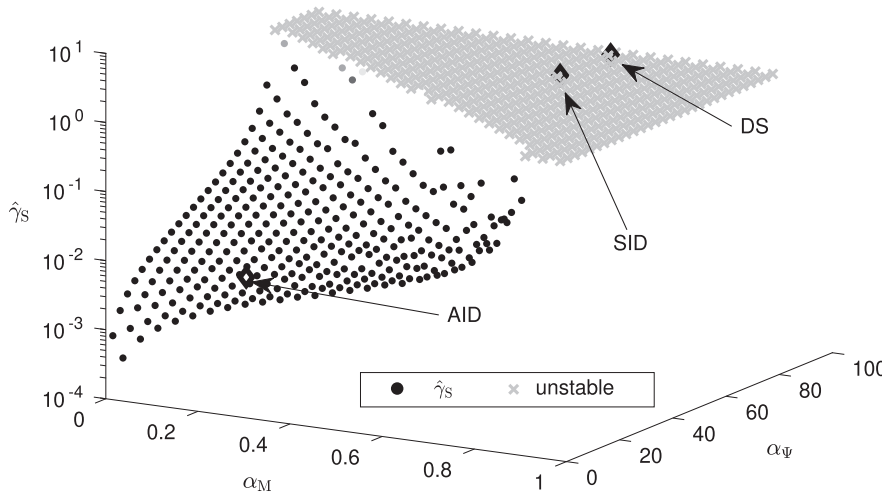

FIGURE 7 Evaluation of worst-case $\|S\|_\infty$ over a grid of both α_Ψ and α_M, where unstable S are marked by x. There is a relatively clear boundary between overall acceptable worst-case model uncertainty and a nonrobust nominal control loop with the gains (43) in the outer loop. The depicted inner-loop controllers AID, SID, and DS are according to Table C1. Here, only the AID allows for robustly stable controller enhancement by some parameter Q. AID, approximate inverse dynamics; DS, diagonal scaling; SID, simplified inverse dynamics

using controller (43). Figures 6 and 7 demonstrate how the main result allows to quantify the worst-case uncertainty set under a given AID situation.

5.1.3 | Influence of nominal outer-loop controller K_0

Central feedback gains. A high-gain PD controller is working robustly in practice to control the rigid manipulator.[37] It is also clear from (33) that the P- and D-gains of the nominal controller influence the uncertainty expressed by the dual-Youla parameter. Hence, we calculated the values of $\hat{\gamma}_S$ over a grid of P/D combinations for the central gain (42). As shown in Figure 8, the evaluation was performed over a dense grid with values of $0 < K_p < 5 \cdot 10^4$ and $0 < K_d < 10^4$. Three different parameter sweeps were performed, with the uncertainty levels α_M and α_Ψ set corresponding to the inner-loop controllers AID, SID, and DS from Table C1. In accordance to intuition, one can observe that the uncertainty in the closed loop decreases with increasing gains and increasing model accuracy. Furthermore, a minimum D-gain of approximately $K_d > 10$ is needed to conclude robust stability although the model employed in the AID controller is relatively good. Note that even if the model had been perfect, some $K_d > 0$ would have been required as lead compensation for the double integrator plant. In accordance to the literature,[37] large PD gains are required for robustification in case of limited model knowledge.

Feedforward term. The previous analysis only considered a controller feeding back position and velocity errors. Here, the effect of adding feedforward terms is examined, ie, $K_{ff} \neq 0$ in (42). In the robust robot controllers of other works,[2,5,9] the outer-loop controller (20) and (23) includes a summand $\ddot{q}_d$. In the ideal case then, $q = \int \int \ddot{q}_d dt^2 = q_d$ even without feedback. In the methods reviewed in Section 2.5, the robust control term v also depends on the maximum norm $\|\ddot{q}_d\|_{\mathcal{L}_\infty}$ of the desired trajectory acceleration. In the framework put forward in this article, on the contrary, the uncertainty measure S does not change when the feedforward gains are included in (42) by some $K_{ff} \neq 0$. This may
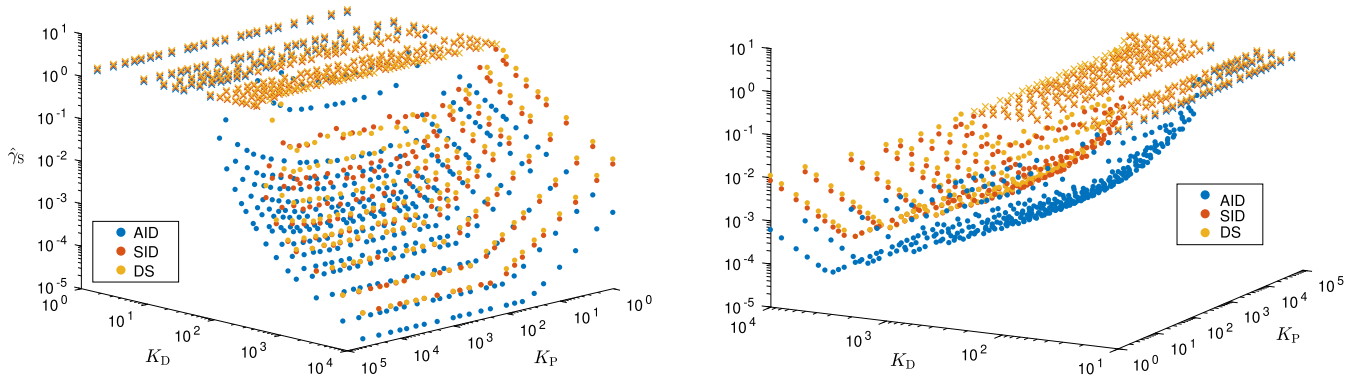
FIGURE 8 Evaluation of worst-case $\|S\|_\infty$ over a grid of P- and D-gains in the outer loop, given the three inner-loop controllers AID, SID, and DS according to Table C1. Configurations where $\hat\gamma_S$ is not finite are marked by x for visibility. The GC and NID controllers yield unstable S everywhere on the depicted grid and are hence excluded from the graph. The PFL case is also not depicted as $\hat\gamma_S = 0, \forall K_d, K_p > 0$. AID, approximate inverse dynamics; DS, diagonal scaling; GC, gravity compensation; NID, no inverse dynamics; PFL, perfect feedback linearization; SID, simplified inverse dynamics [Colour figure can be viewed at wileyonlinelibrary.com]

seem counterintuitive, but it is a simple consequence of the clear structure obtained by the generalized plant: Due to the Q-parameterization, subsequent controller design is based on an internal model of the plant; hence, the structure is carried into all controllers parameterized by Q (cf Remark 2). More formally, a two-DoF controller can be thought of as a single controller $K = [K_{ff}, K_{fb}]$ in feedback connection with an augmented plant $[0, G^\top]^\top$.[22(p32f)] Hence, all two-DoF controllers stabilizing G are obtained,[22(pp49f,53)] as all one-DoF controllers for $[0, G^\top]^\top$. Consequently, the plant in feedforward control channels is known *exactly*: It is a zero operator. The control $\boldsymbol{u}$ cannot affect feedforward signals. Naturally, the associated uncertainty with this plant is zero, as are the corresponding entries in $S = \begin{bmatrix} S_{fb} \\ S_{ff} \end{bmatrix} = \begin{bmatrix} S_{fb} \\ 0 \end{bmatrix}$. Indeed, in our example system with the measurements according to Remark 7, calculating the uncertain operator $S(\Delta)$ confirms that its realization always has the form

$$S : \begin{bmatrix} \boldsymbol{A}_S(\Delta) & \boldsymbol{B}_S(\Delta) \\ \hline \boldsymbol{I}_{4\times4}\boldsymbol{0}_{4\times6} & \boldsymbol{0}_{10\times2} \\ \boldsymbol{0}_{6\times10} & \end{bmatrix}.$$

There is accordingly no uncertainty associated with the last six components of $\boldsymbol{y}$, ie, $\boldsymbol{q}_d, \dot{\boldsymbol{q}}_d, \ddot{\boldsymbol{q}}_d$. It is a clear advantage of the proposed parameterization that the loop uncertainty measure γ_S can be made independent from quantities such as $\boldsymbol{q}_d, \ddot{\boldsymbol{q}}_d$ by the two-DoF design according to Remark 7. Note that Figure 8 is obtained irrespectively of $\boldsymbol{K}_{ff}$ because $\|S\|_\infty = \|S_{fb}\|_\infty$.

5.2 | Illustrative example: P560 with varying payload

With the previous example, only the novel dual-Youla perspective on AID uncertainty was discussed. In this section, the utilization of the complete double-Youla parameterization is illustrated by means of a multi-DoF robot system under varying payload. To this end, we consider a PUMA P560 manipulator with six DoF, the dynamic model being publicly available from the work of Corke.[57] The task is to track a fast reference trajectory for each joint while the payload m_p applied in 10 cm distance to the end-effector is uncertain within $m_p \in [0.5, 1.5]$ kg. The trajectory is chosen to cross areas of the state-space where nonlinearities and inertial interactions are strong; precisely, we use $\boldsymbol{q}_{d,i}(t) = q_{0,i} + a_i \frac{\pi}{180} \sin(2\pi f_i t)$, where $a_1 = 90, a_2 = 45, a_3 = 22.5, a_4 = 55, a_5 = 50, a_6 = 133$ and $f_1 = 0.2, f_2 = 0.4, f_3 = 1, f_4 = 0.5, f_5 = 0.25, f_6 = 0.2$. Let us walk trough steps ①–⑤ of our approach as summarized in Section 4.

① For the nominal control design, an inverse dynamics controller is used in the inner loop based on the robot model for $m_{nom} = 1.0$ kg. Given the varying payload, this controller can only achieve an approximate feedback linearization. Therefore, an outer-loop controller K_0 is designed to robustify the loop. We use the proportional gains $K_p = 900$ and derivative gains $K_d = 2\sqrt{K_p} = 60$ in each joint.

② Next, one needs to obtain numeric values for the bounds (9), (10), and (A1a). By a simulation as in the work of Rocco,[13] we find

$$\alpha = 0.3438 \quad \text{(worst case with } m_{\text{p}} = 0.5), \quad \alpha_0 = 5.4028, \quad \alpha_1 = 4.3689, \quad M_{\text{u}} = 5.7032.$$

③ While the previous bounds are only due to the manipulator and uncertain feedback linearization, we now construct the novel generalized plant setup proposed in Theorem 1. Just as in the previous example, we use the two-DoF design structure given in Appendix C. Now, the uncertainties are conceptually pulled out as shown in Figure 4. To keep the conservatism reasonable, some characteristics of the manipulator are considered. In particular,

- all six DoFs of the P560 are rotational (cf Remark 8);
- the Coriolis and centripetal effects of the P560 are to a very large extent determined from $\dot{q}_1, \dot{q}_2, \dot{q}_3$;
- Friction is independent of payload, hence compensated by the inverse dynamics controller.

Accordingly, the uncertainty structure (28) is described by matrices $\mathbf{\Delta}_{\text{M}} \in \mathbb{R}^{6 \times 6}$ and $\mathbf{\Delta}_{\Psi} \in \mathbb{R}^{3 \times (3+1)}$. From the values obtained in step ②, we have as of (B3) the associated norm bounds $\alpha_{\text{M}} = 0.3438$ and $\alpha_{\Psi} = 39.627$.

④ Next, the realization of the uncertain dual-Youla operator (39) is calculated. We then assign the probability levels $p = 99.9\%$ and $\delta = 10^{-4}$ to employ Algorithm 1 from Table 1, using 10^4 samples. The worst estimate is $\hat{\gamma}_{\text{S}} = 0.1137$.

⑤ The detailed uncertainty quantification of the dual-Youla parameter S by ①-④ is worthwhile once the Q-parameterization is used to enhance performance. That is, the nominal PD controller is firstly augmented, as shown in Figure 5. According to Theorem 3, the parameterization now allows to search over robustly stabilizing controllers simply by choosing a (possibly time-varying) finite-gain $\mathcal{L}_2$ stable parameter system Q. By the value of $\hat{\gamma}_{\text{S}} = 0.1137$, robust stability is assured if $\|Q\|_{\infty} < 1/\hat{\gamma}_{\text{S}} \approx 8.8$.

There is a multitude of design methods for the parameter Q, and the reader is referred to the literature.[15-17,19,21,22,24] Controller design in Q is beyond the scope of this article, yet in general, the less restricted $\|Q\|_{\infty}$ needs to be, the more design freedom there is for any such method.

Let us briefly illustrate this trade-off. To this end, some controllers Q are "designed" by randomly sampling stable dynamic systems of maximum order 10. We run 20 times 50 nonlinear simulations of the closed loop over $T = 10$ seconds, each time increasing the allowed threshold of the loop norm $\|Q\|_{\infty} \cdot \hat{\gamma}_{\text{S}}$ in a logarithmic range of $0.05, 0.1, 0.25, 0.75, \ldots, 500, 10^3, 10^4$. To account for the uncertain load, a random value $0.5 \leq m_{\text{p}} \leq 1.5$ is assigned to the payload in each simulation run. The initial state is $\mathbf{q}_0 = [0, \pi/4, -\pi/2, 0, 0, 0, \mathbf{0}_{1 \times 6}]^{\top}$. A discrete-time formulation of the controller is used for implementation. The sampling time is constant with $t_{\text{s}} = 5$ ms, and the solutions are obtained by a third-order Runge-Kutta method (Bogacki-Shampine). To keep the comparison irrespective of feedforward control, only a feedback controller augmentation is used in this example, ie, $Q_{\text{ff}} = \mathbf{0}_{6 \times 18}$ in all simulations.

The result of these simulations is summarized in Figure 9, depicting the ℓ_2-norm of the six-dimensional error signals. Controllers on the left side of the vertical dashed line in Figure 9 are within the set $\mathcal{K}_{\text{R}}$ from (36). It can be observed that none of the controllers in $\mathcal{K}_{\text{R}}$ leads to a significant increase in the error norm. Leaving the set of admissible robust controllers, the error norms rapidly increase up to practically useless control behavior and instability of the simulated loops starting from approximately $\|Q\|_{\infty} > 20/\hat{\gamma}_{\text{S}}$. Compared to $Q = 0$, 46 of the 548 controllers $K \notin \mathcal{K}_{\text{R}}$ yield better performance; however, 211 controllers $K \notin \mathcal{K}_{\text{R}}$ lead to instability. This study shows how the parameterization of Theorem 3 is indeed useful: It allows to search exclusively over robustly stabilizing controllers. Robust performance can subsequently be obtained by suitable design of Q subject to $\|Q\|_{\infty} < 1/\hat{\gamma}_{\text{S}}$. Approximately half of the LTI systems Q actually improve the performance of the overall control system in this study, albeit being only randomly sampled. This is depicted in Figure 9B, which shows a magnification of the area marked by the rectangle in the lower left corner of Figure 9A.

5.3 | Comparison to related work

Single primary vs double-Youla parameterization. The robust control of Section 2.5.1 derived in the classic frequency domain Youla parameterization always yields a high-gain dynamic compensator.[9] Here, the parameterization is in state-space and it can be based on both dynamic and static central K_0. Moreover, the conventional approach is lumping all uncertainties in a single term (22) of internal feedback disturbances $\boldsymbol{\eta}$ that must be suppressed. In contrast, the structure (28) proposed in this article more accurately reflects that of AID uncertainty (6)-(8).
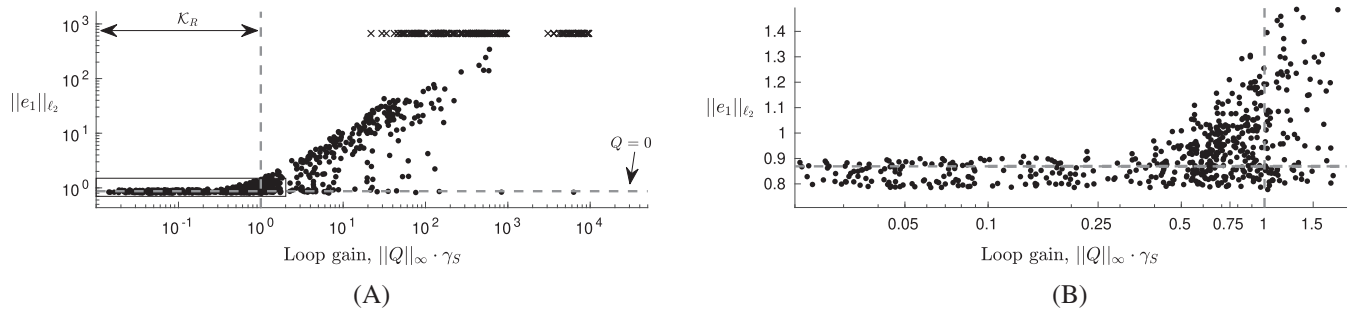
FIGURE 9 Tracking errors of a P560 with uncertain payload and 1000 randomly sampled filters Q. The simulation confirms that all controllers $K(Q) \in \mathcal{K}_R$ robustly stabilize the nonlinear loop. Conservatism is discernible in that some $K(Q) \notin \mathcal{K}_R$ also yield improved performance. A, Joint tracking error norms obtained by 1000 simulation runs with randomly sampled controllers. The gray vertical dashed line denotes the border of the set $\mathcal{K}_R$, ie, $K(Q) \in \mathcal{K}_R$ if $\|Q\|_\infty \hat{\gamma}_S < 1$. The horizontal dashed line depicts the performance of the central PD controller $K(Q = 0)$. Unstable simulations are marked by x. The area in the rectangle is magnified in Figure 9B; B, Performance of 552 randomly sampled controller augmentations, of which 452 fulfill $Q : K(Q) \in \mathcal{K}_R$ (left side of the vertical dashed line). The best such controller improves the tracking performance by 11% w.r.t the nominal design ($Q = 0$) indicated by the horizontal dashed line

It may be less evident that the purpose of the parameterizations is quite different. In the method of Spong and Vidyasagar,[9] the central controller does not ensure robust stability; robustness is obtained by careful design of Q ("The choice of [Q] is not easy to see"[9]). As the primary Youla parameterization only yields stabilizing controllers for the unperturbed plant, ie, the nominal double integrator, in the work of Spong and Vidyasagar,[9] the design of the filter system Q must ensure that the internal disturbance η is suppressed and not destabilizing. In this paper, we do not report another robustification tool but rather characterize a whole set of robustly stabilizing AID controllers (36) such that the control performance can be enhanced online (cf Figure 1 and Remark 5). Such enhancement is possible using time-varying or switching schemes, including adaptive,[23,29] learning,[11] model predictive,[20] hybrid,[21] and gain scheduling[18,19] approaches. Most of these references only focus on the design aspect of the system Q, ie, design for a nominal model within the set of stabilizing controllers. By the contributions in this article, such a design can be systematically tightened to the subset of robustly stabilizing controllers for robot manipulators. Finally, the traditional approach dictates the design of the system Q and is therefore limited to robust trajectory tracking control. The double-Youla framework reported in this article, in general, does not make this restriction because all derivations refer to the generalized plant (25).

Comparison to Lyapunov-based designs. By the revised robust control design, Bascetta and Rocco[5] essentially undo the step in the Lyapunov-based designs (Section 2.5.2) of lumping the closed-loop uncertainty into a single term η in (24). Their method consists of two steps: First, the nominal PD controller is designed to ensure global asymptotic stability of the error system under perturbation with any admissible matrix $\|\Delta_M\| \leq \alpha$. Second, the asymptotic performance under the influence of the neglected terms $\tilde{n}$ is recovered by an additional feedback term $v = f(e)$ obtained via a quadratic Lyapunov function. Our requirement of (35) that robust stability is ensured by the nominal controller is therefore similar to the first step of Bascetta and Rocco.[5] While the methodological approach is quite different, the additional input δu in this paper corresponds to the term v in the work of Bascetta and Rocco,[5] as emphasized in Remark 6. The parameterization of Theorem 3 thus constitutes a viable alternative to the Lyapunov-based methods. The general drawback of a factorization approach is that only uniform ultimate boundedness is ensured as long as the linear bound (10) holds. In turn, the double-Youla parameterization brings some advantages. First, the Lyapunov approaches to robust manipulator control typically result in high-frequency additional control signals v. Here, in contrast, the characteristics of δu depend exclusively on the design of Q. For example, the controllers of Section 5.2 generate smooth signals because Q is LTI. Second, Bascetta and Rocco[5] only deal with robust tracking control. The novel double-Youla parameterization, however, is derived for a generalized plant structure (25) and an arbitrary LTI controller K_0. It therefore complements the Lyapunov-based approaches in terms of versatility, as (25) allows to represent via z many more control objectives in the design step of Q.

Recent approaches. Let us finally recapitulate the distinctive features of the presented double-Youla approach compared to recent literature on robust manipulator control. The conservatism is determined by the accuracy of the model bounds and nominal outer-loop compensator gains. Helwa et al[58] consequently propose a learning-based adjustment of the uncertainty bounds in the Lyapunov-based robust design. Nonetheless, the robustification term is a switching signal of potentially high frequency, and the overall design is tailored towards tracking control; one could then also work with

a robust-adaptive scheme.[59] In addition, the work of Kim et al[46] is related in that the L_1 robustness bounds therein are as well derived by consideration of a generalized plant interconnection. However, Kim et al[46] start from the error system (24), and the disturbance signal is only split into exogenous and internal components. The uncertainty structure used in the work of Kim et al[46] hence does not distinguish between inertia and signal uncertainty, resulting in a conservative design (cf Remark 1). In all these works, the analysis is conducted regardless of the nominal outer-loop PD controller that has considerable influence on robustness. The dual-Youla measure of uncertainty proposed in this article, in turn, provides a general approach to systematically quantify this influence.

6 | CONCLUSION

We provide for the first time a double-Youla parameterization for robust control of rigid body manipulators, with the dual parameterization being the key tool to quantify the uncertainty of the control loop. Using a static nominal controller, the theory specializes to a handy structure suitable for practical implementations. In summary, the proposed methodology constitutes a control strategy that allows to apply numerous advanced design methods for enhancement of inverse dynamics–based feedback controllers in a strict robust stability framework.

We emphasize that the parameterization generally entails controllers based on the internal model principle. Clearly, also the disturbance observer compensation designs are a specific implementation of the internal model principle.[60] Just as the linear robust internal-loop compensator structure from the work of Kim et al[60] has been generalized to the nonlinear setting,[45] a nonlinear flavor of our method might be developed in future work: With suitable extensions,[61] one could take advantage of the available manipulator model directly in terms of a parameterization. It would also be worthwhile to develop a dual-Youla uncertainty characterization for the robust manipulator control with a disturbance observer–based inner loop compensation.[40] Another important research direction is to include the analysis of flexible robots[62] in the framework.

ORCID

Stefan R. Friedrich https://orcid.org/0000-0003-0934-6609
Martin Buss https://orcid.org/0000-0002-1776-2752

REFERENCES

1. Siciliano B, Sciavicco L, Villani L, Oriolo G. *Robotics: Modelling, Planning and Control*. London, UK: Springer; 2009.
2. Sciavicco L, Siciliano B. *Modelling and Control of Robot Manipulators*. London, UK: Springer Science & Business Media; 2012.
3. Spong MW, Hutchinson S, Vidyasagar M. *Robot Modeling and Control*. New York, NY: John Wiley & Sons; 2006.
4. Lewis FL, Dawson DM, Abdallah CT. *Robot Manipulator Control: Theory and Practice*. Boca Raton, FL: CRC Press; 2003.
5. Bascetta L, Rocco P. Revising the robust-control design for rigid robot manipulators. *IEEE Trans Robot*. 2010;26(1):180-187.
6. Youla DC, Jabr H, Bongiorno JJ. Modern Wiener-Hopf design of optimal controllers–part ii: the multivariable case. *IEEE Trans Autom Control*. 1976;21(3):319-338.
7. Kučera V. *Discrete Linear Control: The Polynomial Equation Approach*. New York, NY: John Wiley & Sons; 1979.
8. Anderson BDO. From Youla-Kucera to identification, adaptive and nonlinear control. *Automatica*. 1998;34(12):1485-1506.
9. Spong M, Vidyasagar M. Robust linear compensator design for nonlinear robotic control. *IEEE J Robot Autom*. 1987;3(4):345-351.
10. Vidyasagar M. *Control Systems Synthesis: A Factorization Approach*. Cambridge, MA: MIT Press; 1985.
11. Friedrich SR, Buss M. A robust stability approach to robot reinforcement learning based on a parameterization of stabilizing controllers. Paper presented at: 2017 IEEE International Conference on Robotics and Automation (ICRA); 2017; Singapore.
12. Niemann H. Dual Youla parameterisation. *IEE Proc Control Theory Appl*. 2003;150:493-497.
13. Rocco P. Stability of PID control for industrial robot arms. *IEEE Trans Robot Autom*. 1996;12(4):606-614.
14. Grimm WM. Robot non-linearity bounds evaluation techniques for robust control. *Int J Adaptive Contr Signal Proc*. 1990;4(6):501-522.
15. Zhou K, Doyle JC, Glover K. *Robust and Optimal Control*. Upper Saddle River, NJ: Prentice-Hall; 1996.
16. Dullerud GE, Paganini F. *A Course in Robust Control Theory: A Convex Approach*. New York, NY: Springer-Verlag; 2000.
17. Boyd SP, Barratt CH. *Linear Controller Design: Limits of Performance*. Englewood Cliffs, NJ: Prentice Hall; 1991.

18. Stilwell DJ, Rugh WJ. Stability preserving interpolation methods for the synthesis of gain scheduled controllers. *Automatica*. 2000;36(5):665-671.

19. Bianchi FD, Sánchez-Peña RS. Interpolation for gain-scheduled control with guarantees. *Automatica*. 2011;47(1):239-243.

20. Thomsen SC, Niemann H, Poulsen NK. Robust stability in constrained predictive control through the Youla parameterisations. *Int J Control*. 2011;84(4):653-664.

21. Hespanha JP, Morse AS. Switching between stabilizing controllers. *Automatica*. 2002;38(11):1905-1917.

22. Tay T-T, Mareels I, Moore JB. *High Performance Control*. Boston, MA: Birkhäuser; 1998.

23. Kuipers M, Ioannou P. Multiple model adaptive control with mixing. *IEEE Trans Autom Control*. 2010;55(8):1822-1836.

24. Friedrich SR, Buss M. Direct adaptive-Q control for online performance enhancement of switching linear systems. Paper presented at: 2016 IEEE 55th Conference on Decision and Control (CDC); 2016; Las Vegas, NV.

25. Sugie T, Yoshikawa T, Ono T. Robust controller design for robot manipulators. *J Dyn Syst Meas Control*. 1988;110(1):94-96.

26. Kurfess TR, ed. *Robotics and Automation Handbook*. Boca Raton, FL: CRC press; 2005.

27. Hansen F, Franklin G, Kosut R. Closed-loop identification via the fractional representation: Experiment design. Paper presented at: 1989 American Control Conference (ACC); 1989; Pittsburgh, PA.

28. Oomen T. Advanced motion control for precision mechatronics: control, identification, and learning of complex systems. *IEEJ J Ind Appl*. 2018;7(2):127-140.

29. Tay TT, Moore JB, Horowitz R. Indirect adaptive techniques for fixed controller performance enhancement. *Int J Control*. 1989;50(5):1941-1959.

30. Desoer CA, Vidyasagar M. *Feedback Systems: Input-Output Properties*. New York, NY: Academic Press, Inc; 1975.

31. Douma SG, Van den Hof PMJ, Bosgra OH. Controller tuning freedom under plant identification uncertainty: double Youla beats gap in robust stability. *Automatica*. 2003;39(2):325-333.

32. Evers E, van de Wal M, Oomen T. Beyond decentralized wafer/reticle stage control design: a double-Youla approach for enhancing synchronized motion. *Control Eng Pract*. 2019;83:21-32.

33. Battistelli G, Selvi D, Tesi A. Robust switching control: stability analysis and application to active disturbance attenuation. *IEEE Trans Autom Control*. 2017;62(12):6369-6376.

34. Abdallah C, Dawson DM, Dorato P, Jamshidi M. Survey of robust control for rigid robots. *IEEE Control Syst*. 1991;11(2):24-30.

35. Sage HG, De Mathelin MF, Ostertag E. Robust control of robot manipulators: a survey. *Int J Control*. 1999;72(16):1498-1522.

36. Dawson DM, Qu Z, Lewis FL, Dorsey JF. Robust control for the tracking of robot motion. *Int J Control*. 1990;52(3):581-595.

37. Qu Z, Dorsey J. Robust tracking control of robots by a linear feedback law. *IEEE Trans Autom Control*. 1991;36(9):1081-1084.

38. Kim JH, Hur S-M, Oh Y. Performance analysis for bounded persistent disturbances in PD/PID-controlled robotic systems with its experimental demonstrations. *Int J Control*. 2018;91(3):688-705.

39. Schill MM, Buss M. Kinematic trajectory planning for dynamically unconstrained nonprehensile joints. *IEEE Robot Autom Lett*. 2018;3(2):728-734.

40. Sariyildiz E, Sekiguchi H, Nozaki T, Ugurlu B, Ohnishi K. A stability analysis for the acceleration-based robust position control of robot manipulators via disturbance observer. *IEEE/ASME Trans Mechatronics*. 2018;23(5):2369-2378.

41. Jin M, Kang SH, Chang PH, Lee J. Robust control of robot manipulators using inclusive and enhanced time delay control. *IEEE/ASME Trans Mechatronics*. 2017;22(5):2141-2152.

42. Seraji H. Decentralized adaptive control of manipulators: theory, simulation, and experimentation. *IEEE Trans Robot Autom*. 1989;5(2):183-201.

43. Hu R, Müller PC. Position control of robots by nonlinearity estimation and compensation: theory and experiments. *J Intell Robot Syst*. 1997;20(2):195-209.

44. Kolhe PJ, Shaheed MD, Chandar TS, Talole SE. Robust control of robot manipulators based on uncertainty and disturbance estimation. *Int J Robust Nonlin Control*. 2013;23(1):104-122.

45. Kim MJ, Choi Y, Chung WK. Bringing nonlinear $\mathcal{H}_\infty$ optimality to robot controllers. *IEEE Trans Robot*. 2015;31(3):682-698.

46. Kim JH, Hur S, Oh Y. L_1 robustness of computed torque method for robot manipulators. In: 2018 IEEE International Conference on Robotics and Automation (ICRA); 2018; Brisbane, Australia.

47. Pchelkin SS, Shiriaev AS, Robertsson A, et al. On orbital stabilization for industrial manipulators: case study in evaluating performances of modified PD+ and inverse dynamics controllers. *IEEE Trans Control Syst Technol*. 2017;25(1):101-117.

48. Canudas de Wit C, Siciliano B, Bastin G, eds. *Theory of Robot Control*. London, UK: Springer; 1996.

49. Skogestad S, Postlethwaite I. *Multivariable Feedback Control: Analysis and Design*. New York, NY: John Wiley & Sons; 2005.

50. Petersen IR, Tempo R. Robust control of uncertain systems: classical results and recent developments. *Automatica*. 2014;50(5):1315-1335.

51. Niemann H, Stoustrup J. An architecture for implementation of multivariable controllers. In: Proceedings of the 1999 American Control Conference (ACC); 1999; San Diego, CA.

52. Balas GJ, Packard AK, Safonov MG, Chiang RY. Next generation of tools for robust control. In: Proceedings of the 2004 American Control Conference (ACC); 2004; Boston, MA.

53. Young PM, Newlin MP, Doyle JC. Mu analysis with real parametric uncertainty. In: Proceedings of the 30th IEEE Conference on Decision and Control (CDC); 1991; Brighton, UK.

54. Packard A, Balas G, Liu R, Shin J-Y. Results on worst-case performance assessment. In: Proceedings of the 2000 American Control Conference (ACC); 2000; Chicago, IL.

55. Tempo R, Calafiore G, Dabbene F. *Randomized Algorithms for Analysis and Control of Uncertain Systems*. London, UK: Springer; 2004.

56. Tremba A, Calafiore G, Dabbene F, et al. RACT: randomized algorithms control toolbox for MATLAB. *IFAC Proc Vol*. 2008;41:390-395.

57. Corke PI. *Robotics, Vision and Control: Fundamental Algorithms in MATLAB*. Berlin, Germany: Springer; 2011.

58. Helwa MK, Heins A, Schoellig AP. Provably robust learning-based approach for high-accuracy tracking control of Lagrangian systems. *IEEE Robot Autom Lett*. 2019;4(2):1587-1594.

59. Hayat R, Leibold M, Buss M. Robust-adaptive controller design for robot manipulators using the $\mathcal{H}_\infty$ approach. *IEEE Access*. 2018;6:51626-51639.

60. Kim BK, Choi HT, Chung WK, Suh IH. Analysis and design of robust motion controllers in the unified framework. *ASME J Dyn Syst Meas Control*. 2002;124(2):313-320.

61. Aliyu MDS. *Nonlinear H-Infinity Control, Hamiltonian Systems and Hamilton-Jacobi Equations*. Boca Raton, FL: CRC Press; 2011.

62. Liu Z, Liu J, He Wei. Dynamic modeling and vibration control for a nonlinear 3-dimensional flexible manipulator. *Int J Robust Nonlinear Control*. 2018;28(13):3927-3945.

63. Khalil HK. *Nonlinear Systems*. 3rd ed. Upper Saddle River, NJ: Pearson Education Limited; 2002.

64. Ishihara JY, Sales RM. Doubly coprime factorizations related to any stabilizing controllers in state space. *Automatica*. 1999;35(9):1573-1577.

APPENDIX A

STANDARD ROBOTIC NORM BOUNDS

The reader is referred to other works[2,4,9] for details and an in-depth interpretation of the following assumptions.

Assumption 2 (Manipulator dynamic bounds[2,4]). When the robot arm (1) is revolute, there exist known positive constants M_l, M_u, C_u, F_u, and g_u such that, for all $(t, \boldsymbol{q}, \dot{\boldsymbol{q}}) \in \mathbb{R}^t \times \mathbb{R}^n \times \mathbb{R}^n$, the matrices $\boldsymbol{M}(\boldsymbol{q})$, $\boldsymbol{C}(\boldsymbol{q}, \dot{\boldsymbol{q}})$ and the vectors $\boldsymbol{f}(\dot{\boldsymbol{q}})$ and $\boldsymbol{g}(\boldsymbol{q})$ satisfy the following inequalities:

$$0 < M_l \leq \|\boldsymbol{M}(\boldsymbol{q})^{-1}\| \leq M_u < \infty, \tag{A1a}$$

$$\|\boldsymbol{C}(\boldsymbol{q}, \dot{\boldsymbol{q}})\| \leq C_u\|\dot{\boldsymbol{q}}\|, \quad \|\boldsymbol{F}(\dot{\boldsymbol{q}})\| \leq F_u\|\dot{\boldsymbol{q}}\|, \quad \|\boldsymbol{g}(\boldsymbol{q})\| \leq g_u. \tag{A1b}$$

The workspace of the manipulator is bounded $\|\boldsymbol{q}\|_{\mathcal{L}_\infty} \leq q_{\max}$; hence, the inertia matrix $\boldsymbol{M}(\boldsymbol{q})$ is invertible for all $\boldsymbol{q}$. Finally, $\|\dot{\boldsymbol{q}}\|_{\mathcal{L}_\infty} \leq v_{\max}$ holds due to the power limitation.

Assumption 3 (Exogenous signal bounds).

1. The input disturbance is bounded from above by a known constant C_{dist} such that $\|\boldsymbol{\tau}_{\text{dist}}\|_{\mathcal{L}_\infty} \leq C_{\text{dist}} < \infty$.
2. The measurement noise fulfills $\|\boldsymbol{w}_i\|_{\mathcal{L}_\infty} \leq W_i$, $i = 1, 2$, for some known constants $W_i < \infty$.
3. The reference trajectory satisfies $\|\boldsymbol{q}_d\|_{\mathcal{L}_\infty} \triangleq Q_d$.

APPENDIX B

PROOFS

The following simple auxiliary inequality is introduced.

Lemma 2. *Let $a_1, a_2 \in \mathbb{R}$ and $\boldsymbol{h}_1, \boldsymbol{h}_2 \in \mathbb{R}^n$; then,*

$$[a_1, a_2]\text{col}(\|\boldsymbol{h}_1\|, \|\boldsymbol{h}_2\|) \leq \|[a_1, a_2]\| \|\text{col}(\boldsymbol{h}_1, \boldsymbol{h}_2)\|. \tag{B1}$$

Proof. (B2) can be shown by straightforward algebraic manipulation and the definition of the induced vector 2-norm. $\square$

B.1 | Proof of Theorem 1

Proof. The state- and control-dependent nonlinear terms of $\boldsymbol{w}_\Delta^\mathrm{U}$ in (27) are collected separately in a vector $\boldsymbol{w}_\Delta = \mathrm{col}(\boldsymbol{w}_\Delta^\mathrm{M} \boldsymbol{w}_\Delta^\Psi)$. We then have

$$\|\boldsymbol{w}_\Delta\| = \left\|\begin{bmatrix} \boldsymbol{w}_\Delta^\mathrm{M} \\ \boldsymbol{w}_\Delta^\Psi \end{bmatrix}\right\| \le \left\|\begin{bmatrix} \|\boldsymbol{\Delta}_\mathrm{M}\boldsymbol{u}\| \\ \|\boldsymbol{M}^{-1}\widetilde{\boldsymbol{n}}\| \end{bmatrix}\right\| \le \left\|\begin{bmatrix} \|\boldsymbol{\Delta}_\mathrm{M}\|\,\|\boldsymbol{u}\| \\ \|\boldsymbol{M}^{-1}\|\,\|\widetilde{\boldsymbol{n}}\| \end{bmatrix}\right\|,$$

where the last inequality is due to the submultiplicative property of compatible induced matrix norms. Inserting the bounds (10) and (A1a) yields

$$\|\boldsymbol{w}_\Delta\| \le \left\|\begin{bmatrix} \|\boldsymbol{\Delta}_\mathrm{M}\|\,\|\boldsymbol{u}\| \\ M_\mathrm{u}\alpha_0 + M_\mathrm{u}\alpha_1\,\|\boldsymbol{x}\| \end{bmatrix}\right\|.$$

At this point, one cannot simply treat the constant part of $\Phi(\|\boldsymbol{x}\|)$ as if it were a bounded additive disturbance $\boldsymbol{w}_\mathrm{ext}$ such that $\|\boldsymbol{w}_\mathrm{ext}\| \le M_\mathrm{u}\alpha_0$, similarly as it could be done with the external disturbances $\boldsymbol{w}_\mathrm{dist}$. Here, such a step would void conservatism because $\|\mathrm{col}(\|\boldsymbol{u}\|, a + \|\boldsymbol{x}\|)\| \not\le \|\mathrm{col}(\|\boldsymbol{u}\|, \|\boldsymbol{x}\|)\| + a$ in general. To proceed nonetheless, introduce a fictitious perturbation signal $z_\Delta^\mathrm{f} \triangleq 1 = \|z_\Delta^\mathrm{f}\|$ to rewrite the sum $M_\mathrm{u}\alpha_0 + M_\mathrm{u}\alpha_1\|\boldsymbol{x}\|$ as a dot product

$$\|\boldsymbol{w}_\Delta\| \le \left\|\begin{bmatrix} \|\boldsymbol{\Delta}_\mathrm{M}\|\|\boldsymbol{u}\| \\ [M_\mathrm{u}\alpha_0, M_\mathrm{u}\alpha_1] \cdot \begin{bmatrix} \|z_\Delta^\mathrm{f}\| \\ \left\|\begin{bmatrix} \boldsymbol{q} \\ \dot{\boldsymbol{q}} \end{bmatrix}\right\| \end{bmatrix} \end{bmatrix}\right\|.$$

By application of Lemma 2, we have

$$\|\boldsymbol{w}_\Delta\| \le \left\|\begin{bmatrix} \|\boldsymbol{\Delta}_\mathrm{M}\|\|\boldsymbol{u}\| \\ \|[M_\mathrm{u}\alpha_0, M_\mathrm{u}\alpha_1]\| \cdot \left\|\begin{bmatrix} z_\Delta^\mathrm{f} \\ \boldsymbol{q} \\ \dot{\boldsymbol{q}} \end{bmatrix}\right\| \end{bmatrix}\right\| = \left\|\begin{bmatrix} \|\boldsymbol{\Delta}_\mathrm{M}\| & 0 \\ 0 & \|[M_\mathrm{u}\alpha_0, M_\mathrm{u}\alpha_1]\| \end{bmatrix} \begin{bmatrix} \|\boldsymbol{u}\| \\ \left\|\begin{bmatrix} z_\Delta^\mathrm{f} \\ \boldsymbol{q} \\ \dot{\boldsymbol{q}} \end{bmatrix}\right\| \end{bmatrix}\right\| \le \left\|\begin{bmatrix} \alpha_\mathrm{M} & 0 \\ 0 & \alpha_\Psi \end{bmatrix}\right\| \cdot \left\|\begin{bmatrix} \boldsymbol{u} \\ z_\Delta^\mathrm{f} \\ \boldsymbol{q} \\ \dot{\boldsymbol{q}} \end{bmatrix}\right\|, \quad \text{(B2)}$$

where the abbreviations

$$\alpha_\mathrm{M} \triangleq \|\boldsymbol{\Delta}_\mathrm{M}\| \overset{(9)}{=} \alpha, \qquad \alpha_\Psi \triangleq \|[M_\mathrm{u}\alpha_0,\ M_\mathrm{u}\alpha_1]\| \tag{B3}$$

are introduced. Denote by $\boldsymbol{z}_\Delta \triangleq \mathrm{col}(\boldsymbol{u}, z_\Delta^\mathrm{f}, \boldsymbol{q}, \dot{\boldsymbol{q}})$ the vector of signals exciting uncertainty. Thus, by the inequality (B2), a conservative gain bound such that $\|\boldsymbol{w}_\Delta\|_{\mathcal{L}_\infty} \le \|\boldsymbol{\Delta}\boldsymbol{z}_\Delta\|_{\mathcal{L}_\infty}$ is given[‡] by $\|\boldsymbol{\Delta}\| \le \|\mathrm{diag}(\alpha_\mathrm{M}, \alpha_\Psi)\| = \max(\alpha_\mathrm{M}, \alpha_\Psi)$, where $\boldsymbol{\Delta} \in \mathbb{R}^{2n\times(3n+1)}$ is any real matrix of appropriate size and norm. From their definitions, however, it is known that $\boldsymbol{w}_\Delta^\mathrm{M}(\boldsymbol{u})$ and $\boldsymbol{w}_\Delta^\Psi(\boldsymbol{q}, \dot{\boldsymbol{q}})$ are decoupled. It follows that the relevant uncertain matrices can be restricted to a set $\mathcal{D}_\Delta$ of block diagonal matrices with separate norm bounds

$$\mathcal{D}_\Delta = \left\{ \boldsymbol{\Delta} = \begin{bmatrix} \boldsymbol{\Delta}_\mathrm{M} & \boldsymbol{0} \\ \boldsymbol{0} & \boldsymbol{\Delta}_\Psi \end{bmatrix} :\ \boldsymbol{\Delta}_\mathrm{M} \in \mathbb{R}^{n\times n}, \boldsymbol{\Delta}_\Psi \in \mathbb{R}^{n\times(2n+1)}, \|\boldsymbol{\Delta}_\mathrm{M}\| \le \alpha_\mathrm{M}, \|\boldsymbol{\Delta}_\Psi\| \le \alpha_\Psi \right\}.$$

$\square$

B.2 | Proof of Theorem 2

Proof. Begin by checking that $(\boldsymbol{A}_{11}, \boldsymbol{B}_{13})$ is stabilizable and $(\boldsymbol{A}_{11}, \boldsymbol{C}_{31})$ detectable, which can be easily verified for the generalized plant given by (C1) to (C2). Furthermore, $\boldsymbol{D}_{33} = 0$, ie, there is no direct feedthrough in the control channel

---

[‡]Note that the spatial norm in the definition of the $\mathcal{L}_\infty$-norm can be any vector p-norm[63]; here, $p = 2$.

of the plant. Then, for the general controller (31), a coprime factorization can be obtained directly in state-space by adopting the formulae given in the works of Tay et al[29] and Ishihara and Sales[64]

$$
\begin{bmatrix} M_0 & U_0 \\ N_0 & V_0 \end{bmatrix} : \left[\begin{array}{cc|cc} A_{11}+B_{13}F_G & 0 & B_{13} & 0 \\ 0 & A_K+B_KF_K & 0 & B_K \\ \hline F_G & C_K+D_KF_K & I & D_K \\ C_{31} & F_K & 0 & I \end{array}\right], \quad \begin{bmatrix} \tilde{V}_0 & -\tilde{U}_0 \\ -\tilde{N}_0 & \tilde{M}_0 \end{bmatrix} : \left[\begin{array}{cc|cc} A_{11}+B_{13}D_KC_{31} & B_{13}C_{11} & -B_{13} & B_{13}D_K \\ B_KC_{31} & A_K & 0 & B_K \\ \hline F_G-D_KC_{31} & -C_K & I & -D_K \\ C_{31} & -F_K & 0 & I \end{array}\right] \quad \text{(B4)}
$$

Next, an expression for T_Δ from (30) has to be calculated, which we repeat here for convenience:

$$
\begin{bmatrix} T_{\Delta,11} & T_{\Delta,12} \\ T_{\Delta,21} & T_{\Delta,22} \end{bmatrix} = \begin{bmatrix} G_{z_\Delta w_\Delta}+G_{z_\Delta u}U_0\tilde{M}_0 G_{yw_\Delta} & G_{z_\Delta u}M_0 \\ \tilde{M}_0 G_{yw_\Delta} & 0 \end{bmatrix}.
$$

Let us also explicitly state the following systems determined from (C1) as

$$
G_{z_\Delta w_\Delta} : \left[\begin{array}{c|c} A_{11} & B_{11} \\ \hline C_{11} & D_{11} \end{array}\right], \quad G_{yw_\Delta} : \left[\begin{array}{c|c} A_{11} & B_{11} \\ \hline C_{31} & D_{31} \end{array}\right], \quad G_{z_\Delta u} : \left[\begin{array}{c|c} A_{11} & B_{13} \\ \hline C_{11} & D_{13} \end{array}\right].
$$

The steps to obtain a compact expression of $T_{\Delta,11}$ are the insertion of the coprime factors U_0 and $\tilde{M}_0$ from (B4) and algebraic simplification, subsequent application of a state similarity transformation such that $\xi = \overline{T}x$ with

$$
\overline{T} = \begin{bmatrix} I & I & 0 & 0 & 0 & 0 & 0 \\ 0 & 0 & 0 & I & 0 & 0 & 0 \\ 0 & -I & 0 & 0 & I & 0 & 0 \\ 0 & 0 & I & 0 & 0 & 0 & 0 \\ I & 0 & 0 & 0 & 0 & 0 & 0 \\ 0 & 0 & 0 & -I & 0 & I & 0 \\ -I & 0 & 0 & 0 & 0 & 0 & I \end{bmatrix}.
$$

and the removal of four uncontrollable and one unobservable modes. A realization is finally obtained as

$$
T_{\Delta,11} : \left[\begin{array}{cc|c} A_{11}+B_{13}D_KC_{31} & B_{13}C_{11} & B_{13}D_KD_{31}+B_{11} \\ B_KC_{31} & A_{11} & B_KD_{31} \\ \hline D_{13}D_KC_{31}+C_{11} & D_{13}C_K & D_{13}D_KD_{31}+D_{11} \end{array}\right]
$$

By analogous steps, for $T_{\Delta,12}$ and $T_{\Delta,21}$, we have

$$
T_{\Delta,12} : \left[\begin{array}{c|c} A_{11}+B_{13}F_G & B_{13} \\ \hline D_{13}F_G+C_{11} & D_{13} \end{array}\right] \quad \text{and} \quad T_{\Delta,12} : \left[\begin{array}{cc|c} A_{11}+B_{13}D_KC_{31} & B_{13}C_{11} & B_{13}D_KD_{31}+B_{11} \\ B_{11}C_{31} & A_{11} & B_KD_{31} \\ \hline C_{31} & -F_K & D_{31} \end{array}\right],
$$

where one uncontrollable and one unobservable mode were removed, respectively. Consequently, assuming $\Delta \triangleq \Delta$ as a nondynamic matrix and defining $\tilde{D} = I - D_{11}\Delta - D_{13}D_KD_{31}\Delta$, a realization for $(I - T_{\Delta,11}\Delta)^{-1}$ is

$$
(I - T_{\Delta,11}\Delta)^{-1} : \left[\begin{array}{c|c} \bar{A} & \bar{B} \\ \hline \bar{C} & \bar{D} \end{array}\right], \quad \text{(B5)}
$$

where

$$
\bar{A} = \begin{bmatrix} \bar{A}_{11} & \bar{A}_{12} \\ \bar{A}_{21} & \bar{A}_{22} \end{bmatrix},
$$

$$
\bar{A}_{11} = B_{13}D_KC_{31}+B_{11}\Delta\tilde{D}^{-1}C_{11}+B_{11}\Delta\tilde{D}^{-1}D_{13}D_KC_{31}+B_{13}D_KD_{31}\Delta\tilde{D}^{-1}C_{11}+B_{13}D_KD_{31}\Delta\tilde{D}^{-1}D_{13}D_KC_{31}+A_{11},
$$

$$
\bar{A}_{12} = B_{13}C_K+B_{11}\Delta\tilde{D}^{-1}D_{13}C_K+B_{13}D_KD_{31}\Delta\tilde{D}^{-1}D_{13}C_K,
$$

$$
\bar{A}_{21} = B_KC_{31}+B_KD_{31}\Delta\tilde{D}^{-1}C_{11}+B_KD_{31}\Delta\tilde{D}^{-1}D_{13}D_KC_{31}, \qquad \bar{A}_{22} = A_K+B_KD_{31}\Delta\tilde{D}^{-1}D_{13}C_K,
$$

$$
\bar{B} = \begin{bmatrix} B_{11}\Delta\tilde{D}^{-1}-B_{13}D_KD_{31}\Delta\tilde{D}^{-1} \\ -B_KD_{31}\Delta\tilde{D}^{-1} \end{bmatrix}, \qquad \bar{C} = [-\tilde{D}^{-1}C_{11}-\tilde{D}^{-1}D_{13}D_KC_{31}-\tilde{D}^{-1}D_{13}C_K], \qquad \bar{D} = \tilde{D}^{-1}.
$$

Finally, plugging the above realizations of $T_{\Delta,12}$, $(I - T_{\Delta,11}\Delta)^{-1}$ and $T_{\Delta,21}$ into (29) and a number of straightforward but tedious simplifications yield the result (33). $\qquad\square$

B.3 | Proof of Lemma 1

Proof. To obtain a robustly stable loop, the stability condition on (Q, S) from Proposition 4 is not sufficient yet because it only refers to the controlled channel; in Figure 3B, however, the prestabilized yet uncertain loop $T(S)$ is subject to exogenous inputs $\boldsymbol{w}$. Hence, to ensure robust closed-loop internal stability, it is required that the pair $\left(\begin{bmatrix} 0 & 0 \\ 0 & Q \end{bmatrix}, T(S) \right)$ be stable[22(p80)] for all allowed perturbations. To this end, it is sufficient to show[22(p32)] that $T_{11}(S), T_{12}(S), T_{21}(S) \in \mathcal{RH}_\infty$ as $S \in \mathcal{RH}_\infty$, and $(Q, T_{22}(S)) = (Q, S)$ should be a stabilizing loop by construction. Denoting with $P(S)$ the transfer matrix between $\mathrm{col}(\boldsymbol{w}, \boldsymbol{u})$ and $\mathrm{col}(\boldsymbol{z}, \boldsymbol{y})$ for the plant determined by S, the uncertain operator $T(S)$ is given by[22(p79)]

$$T(S) = \begin{bmatrix} T_{11}(S) & T_{12}(S) \\ T_{21}(S) & T_{22}(S) \end{bmatrix} = \begin{bmatrix} P_{11}(S) + P_{12}(S)U\tilde{M}(S)P_{21}(S) & P_{12}(S)M(S) \\ \tilde{M}(S)P_{21}(S) & S \end{bmatrix}. \tag{B6}$$

By the first condition (i), consider that (35) is necessary and sufficient for the stability of the nominal uncertain loop. Then, for all $\Delta \in \mathcal{D}_\Delta$, there exists a stable dual-Youla operator $S \in \mathcal{RH}_\infty$ whose coprime factors satisfy $\tilde{M}(S), M(S) \in \mathcal{RH}_\infty$ by construction and consequently $S_\Delta \subset \mathcal{RH}_\infty$. Using (29) to calculate S, by the factorization, the plant under control $P(S)$ in (B6) is precisely that of the uncertain plant $\mathcal{F}_u(G, \Delta)$ from the controller's point of view. Thus, with (35) also $P_{11}(S), P_{12}(S), P_{21}(S) \in \mathcal{RH}_\infty$ and consequently $T(S) \in \mathcal{RH}_\infty \forall \Delta \in \mathcal{D}_\Delta$. Alternatively, the requirement (i) could also be proved by coprimeness of the factors involved (App. B in the work of Thomsen et al[20]). The requirement (ii) follows directly from the small-gain condition of Proposition 4: S is an uncertain stable time-varying operator and the only assumption about the plug-in controller Q is that $\|Q\|_\infty \leq \gamma_Q$ for some finite γ_Q. The small-gain theorem is therefore necessary (Th. 9.1 in the work of Zhou et al[15]) to ensure that all $S \in S_\Delta$ are stabilized by all $Q \in Q$. $\qquad\square$

APPENDIX C

STATE-SPACE REALIZATION OF GENERALIZED PLANT FOR TRACKING CONTROL

A state-space description of (25) is

$$G : \begin{bmatrix} \boldsymbol{A}_{11} & \boldsymbol{B}_{11} & \boldsymbol{B}_{12} & \boldsymbol{B}_{13} \\ \hline \boldsymbol{C}_{11} & \boldsymbol{D}_{11} & \boldsymbol{D}_{12} & \boldsymbol{D}_{13} \\ \boldsymbol{C}_{21} & \boldsymbol{D}_{21} & \boldsymbol{D}_{22} & \boldsymbol{D}_{23} \\ \boldsymbol{C}_{31} & \boldsymbol{D}_{31} & \boldsymbol{D}_{32} & \boldsymbol{0} \end{bmatrix}, \tag{C1}$$

with $(\boldsymbol{A}_{11}, \boldsymbol{B}_{13})$ and $(\boldsymbol{A}_{11}, \boldsymbol{C}_{31})$ stabilizable and detectable pairs, respectively. For the case of a two-DoF tracking control design (Figure 4 specialized according to Remark 7 and Remark 8), we have

$$\boldsymbol{A}_{11} = \begin{bmatrix} \boldsymbol{0}_n & \boldsymbol{I}_n \\ \boldsymbol{0}_n & \boldsymbol{0}_n \end{bmatrix}, \boldsymbol{B}_{11} = \begin{bmatrix} \boldsymbol{0}_n & \boldsymbol{0}_n \\ \boldsymbol{I}_n & \boldsymbol{I}_n \end{bmatrix}, \boldsymbol{B}_{12} = \begin{bmatrix} \boldsymbol{0}_{n\times(5n+1)} & \boldsymbol{0}_n \\ \boldsymbol{0}_{n\times(5n+1)} & \boldsymbol{I}_n \end{bmatrix}, \boldsymbol{B}_{13} = \begin{bmatrix} \boldsymbol{0}_n \\ \boldsymbol{I}_n \end{bmatrix}, \boldsymbol{C}_{11} = \begin{bmatrix} \boldsymbol{0}_{(n+1)\times 2n} \\ \boldsymbol{0}_n & \boldsymbol{I}_n \end{bmatrix}, \boldsymbol{C}_{21} = \begin{bmatrix} \boldsymbol{I}_n & \boldsymbol{0}_n \\ \boldsymbol{0}_{n\times 2n} \\ \boldsymbol{I}_n & \boldsymbol{0}_n \end{bmatrix},$$

$$\boldsymbol{C}_{31} = \begin{bmatrix} \boldsymbol{I}_{2n} \\ \boldsymbol{0}_{3n\times 2n} \end{bmatrix}, \boldsymbol{D}_{11} = \boldsymbol{0}_{(2n+1)\times 2n}, \boldsymbol{D}_{12} = \begin{bmatrix} \boldsymbol{0}_{n\times(6n+1)} \\ 1 & \boldsymbol{0}_{1\times 6n} \\ \boldsymbol{0}_{n\times(6n+1)} \end{bmatrix}, \boldsymbol{D}_{13} = \begin{bmatrix} \boldsymbol{I}_n \\ \boldsymbol{0}_{(n+1)\times n} \end{bmatrix}, \boldsymbol{D}_{21} = \boldsymbol{0}_{3n\times 2n}, \boldsymbol{D}_{22} = \begin{bmatrix} \boldsymbol{0}_{n\times 1} & -\boldsymbol{I}_n & \boldsymbol{0}_{n\times 5n} \\ \boldsymbol{0}_{2n\times(6n+1)} \end{bmatrix},$$

$$\boldsymbol{D}_{23} = \begin{bmatrix} \boldsymbol{0}_n^\top, \boldsymbol{I}_n^\top, \boldsymbol{0}_n^\top \end{bmatrix}^\top, \boldsymbol{D}_{31} = \boldsymbol{0}_{5n\times 2n}, \boldsymbol{D}_{32} = \begin{bmatrix} \boldsymbol{0}_{2n\times 1} & \boldsymbol{0}_{2n\times 3n} & \boldsymbol{I}_{2n} & \boldsymbol{0}_{2n\times n} \\ \boldsymbol{0}_{3n\times 1} & \boldsymbol{I}_{3n} & & \boldsymbol{0}_{3n} \end{bmatrix}. \tag{C2}$$

TABLE C1 Common cases of control laws employed in the inner approximate inverse dynamics loop (3) and illustrative numeric parameters used in the simulation study, with the values of the uncertainty bounds according to Theorem 1

Type	Inner controller Abbreviation	Inertia estimate $\hat{M}(q)$	Nonlinearities	Bounds α_M	α_ψ
Perfect feedback linearization	PFL	M	$\hat{C}=C, \ \hat{f}=f, \ \hat{g}=g$	0	0
Approximate inverse dynamics	AID	$\begin{bmatrix} 0.17\cos(q_2)+0.702 & 0.0852\cos(q_2)+0.178 \\ 0.0852\cos(q_2)+0.178 & 0.437 \end{bmatrix}$	$\hat{C} = \begin{bmatrix} -0.0852\dot{q}_2\sin(q_2) & -0.0852\sin(q_2)(\dot{q}_1+\dot{q}_2) \\ 0.0852\dot{q}_1\sin(q_2) & 0 \end{bmatrix}$ $\hat{g} = \begin{bmatrix} 4.07\cos(q_1+q_2)+8.87\cos(q_1) \\ 4.07\cos(q_1+q_2) \end{bmatrix}$ $\hat{f} = \text{blkdiag}(4.50, 4.50)\dot{q}$	0.2523	9.092
Simplified inverse dynamics	SID	diag(0.655, 0.356)	$\hat{C}=0, \ \hat{f}=0, \ \hat{g}=g$	0.6457	59.37
Diagonal scaling	DS	diag(0.655, 0.356)	$\hat{C}=0, \ \hat{f}=0, \ \hat{g}=0$	0.6457	77.99
Gravity compensation	GC	I	$\hat{C}=0, \ \hat{f}=0, \ \hat{g}=g$	2.765	59.37
No inverse dynamics	NID	I	$\hat{C}=0, \ \hat{f}=0, \ \hat{g}=0$	2.765	77.99